SUPPORTING INFORMATION

Dimerization of Terminal Alkynes Promoted by a Heterobimetallic Zr/Co Complex

Jeffrey W. Beattie, Canning Wang, Hongtu Zhang, Jeremy P. Krogman, Bruce M. Foxman, Christine M. Thomas

Table of Contents

Experimental Section	S3-S8
General Considerations	S3
Reaction of **1** with phenylacetylene at room temperature	S3-S4
Synthesis of **2b**	S4-S5
Synthesis of **3**	S5-S6
Synthesis of **5**	S6-S7
Reaction of **1** with one equivalent of trimethylsiylacetylene	S7
Reaction of **1** with excess phenylacetylene	S8
Figure S1. ^{1}H NMR spectrum of the reaction of PhCCH and **1** at room temperature	S9
Figure S2. $^{31}P\{^{1}H\}$ NMR spectrum of the reaction of PhCCH and **1** at room temperature in C_6D_6.	S10
Figure S3. GC-MS-FID of the reaction of **1** with phenylacetylene at room temperature showing the mass spectrum of the peak corresponding to the *gem* enyne isomer.	S11
Figure S4. GC-MS-FID of the reaction of **1** with phenylacetylene at room temperature showing the mass spectrum of the peak corresponding to the *Z* enyne isomer.	S12
Figure S5. GC-MS-FID of the reaction of **1** with phenylacetylene at room temperature showing the mass spectrum of the peak corresponding to the *E* enyne isomer.	S13
Figure S6. GC-MS-FID of the reaction of **1** with phenylacetylene at low temperature showing the mass spectrum of the peak corresponding to the *E* enyne isomer.	S14
Figure S7. GC-MS-FID of the reaction of the independently synthesized *Z*-1,3,enyne	S15
Figure S8. ^{1}H NMR spectrum of **2b**	S16
Figure S9. $^{31}P\{^{1}H\}$ NMR spectrum of **2b**	S17
Figure S10. $^{13}C\{^{1}H\}$ NMR spectrum of **2b**	S18
Figure S11. ^{1}H – ^{1}H COSY spectrum of **2b**	S19
Figure S12. ^{1}H – ^{13}C HSQC spectrum of **2b**	S20
Figure S13. ^{1}H – ^{1}H NOESY spectrum of **2b**	S21
Figure S14. ^{1}H NMR spectrum of **3**	S22
Figure S15. $^{31}P\{^{1}H\}$ NMR spectrum of **3**	S23
Figure S16. $^{13}C\{^{1}H\}$ NMR spectrum of **3**	S24
Figure S17. ^{1}H – ^{1}H COSY spectrum of **3**	S25

Figure S18. $^{1}H - ^{13}C$ HSQC spectrum of **3**	S26
Figure S19. $^{1}H - ^{1}H$ NOESY spectrum of **3**	S27
Figure S20. ^{1}H NMR spectrum of **5**	S28
Figure S21. $^{31}P\{^{1}H\}$ NMR spectrum of **5**	S29
Figure S22. $^{13}C\{^{1}H\}$ NMR spectrum of **5**	S30
Figure S23. IR spectrum of **5**	S31
Figure S24. $^{31}P\{^{1}H\}$ NMR spectra of the reaction of **1** with one equivalent of TMSCCH, $^{31}P\{^{1}H\}$ NMR spectrum of **3**, and $^{31}P\{^{1}H\}$ NMR spectrum of **1**.	S32
Figure S25. ^{1}H NMR spectrum of extracted polymer from the reaction of **1** with excess PhCCH	S33
Figure S26. IR spectrum of extracted polymer from the reaction of **1** with excess PhCCH	S34
Figure S27. GC-MS-FID of the reaction of **1** with excess phenylacetylene at room temperature.	S35
Table S1. X-Ray Crystallographic Data	S36
Figure S28. Fully labelled displacement ellipsoid representations of **2a**.	S37
X-Ray data collection, solution, and refinement details for **2a**	S37-S38
Figure S29. Fully labelled displacement ellipsoid representations of **5**.	S39
X-Ray data collection, solution, and refinement details for **5**	S39-S40
References	S41

General Methods and Considerations

Unless otherwise noted, all manipulations were carried out under an inert atmosphere using a nitrogen-filled glovebox. Glassware was oven-dried before use. All protio solvents were degassed by sparging with ultra-high purity argon and dried *via* passage through columns of drying agents using a Seca solvent purification system from Pure Process Technologies. Benzene-d_6 and dichloromethane-d_2 were dried over CaH_2 and then degassed *via* repeated freeze–pump–thaw cycles and dried over 4 Å molecular sieves before use. (THF)Zr(NMesP^{i}Pr$_2$)$_3$CoN$_2$ (**1**) and (THF)Zr(NMesP^{i}Pr$_2$)$_3$CoCN^{t}Bu (**4**) were synthesized according to literature procedures.[1-3] Phenylacetylene and trimethylsilylacetylene were purified by drying over CaH_2 for two days, distilled under N_2, degassed *via* repeated freeze–pump–thaw cycles, and stored over 3 Å molecular sieves. (*Z*)-But-1-en-3-yne-1,4-diyldibenzene was synthesized according to a previously reported procedure.[4] All other reagents and solvents were obtained from commercial sources and used without further purification. IR spectra were recorded on a Bruker Tensor II spectrometer controlled by OPUS software. NMR spectra were recorded at ambient temperature unless otherwise stated on a Bruker DPX 400 MHz or Bruker Advance III HD 600 MHz instrument. ^{1}H and ^{13}C NMR chemical shifts were referenced to residual solvent resonances and are reported in ppm. ^{31}P NMR chemical shifts (in ppm) were referenced using an external standard (85% H_3PO_4, 0 ppm). GC-MS-FID data were collected on an Agilent 7890B/5977B GC/MSD with a split to both FID and mass spectrometer detectors using helium as the carrier gas. Elemental microanalyses were performed by Midwest Microlab, Indianapolis, IN.

Experimental Section

Reaction of **1** with phenylacetylene at room temperature

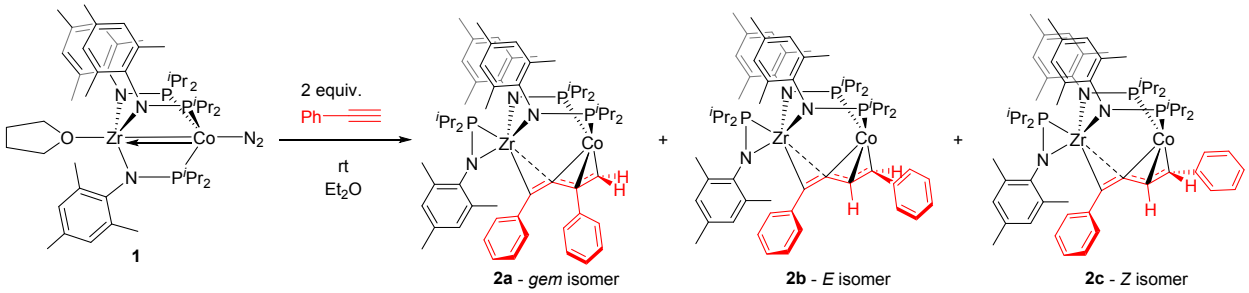

To a stirring solution of **1** (19.9 mg, 0.0199 mmol) in Et_2O (4 mL), phenylacetylene (4.1 µL, 0.37 mmol) was added using a micropipetter. The resulting solution was allowed to stir at room

temperature for 2 hours. The ^{1}H and $^{31}P\{^{1}H\}$ NMR spectra of the reaction mixture at this stage revealed a mixture of products (see Figure S1 and S2). Crystals of **2a** suitable for X-ray crystallographic analysis were grown via concentration of the diethyl ether solution and storage at -35 °C for 48 h. To identify the organic products of alkyne dimerization, the crude reaction mixture was filtered through a pad of silica gel to separate the organics from the metal complex. The resulting solution was diluted and GC-MS-FID analysis revealed formation of the three 1,3-enyne isomers with a gem:*Z:E* ratio of 1:3.5:5.5 (see Figures S3-S6). The peaks in the GC-MS-FID were assigned based on analysis of an authentic sample of the *Z* isomer (Figure S7) in combination with analysis of the isolated complex **2b** that contains the *E* isomer.

Synthesis of **2b**

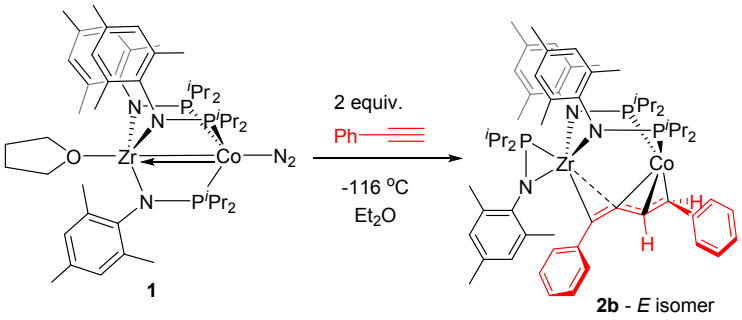

A solution of complex **1** (23.4 mg, 0.0234 mmol) in Et_2O (4 mL) was frozen in the glovebox cold well using liquid N_2. Phenylacetylene (5.0 µL, 0.046 mmol) was added using a micropipetter and the resulting solution was allowed to thaw to room temperature and stir for 2 hours. The solvent was then removed *in vacuo* and the residue was extracted into hexanes (4 mL) and filtered through a pad of Celite. The volatile components were removed from the filtrate *in vacuo,* yielding **2b** as a solid (19.0 mg, 0.0172 mmol, 73.6% yield). ^{1}H NMR (400 MHz, C_6D_6): δ 7.82 (d, 1H, J = 16.0 Hz, R*H*C=CHPh), 7.51 (d, 2H, J = 7.3 Hz, *o*-Ph), 7.47 (d, 2H, J = 7.4 Hz, *o*-Ph), 7.25 (t, 2H J = 7.5 Hz, m-Ph), 7.19 (t overlapping with solvent, 2H, J = 6.5 Hz, *m*-Ph), 7.11 (t, 1H, J = 7.3 Hz, *p*-Ph), 7.04 (t, 1H, J = 7.4 Hz, *p*-Ph), 6.96 (d, 1H, J = 15.8 Hz, RC=C*H*Ph), 6.84 (br s, 2H, Mes), 6.76 (s, 2H, Mes), 6.55 (s, 2H, Mes), 3.75 (m, 1H, PC*H*CH_3), 3.45 (m, 1H, PC*H*CH_3), 2.93-3.96 (overlapping m, 4H, PC*H*CH_3), 2.58 (br s, 6H, MesCH_3), 2.46 (s, 3H, MesCH_3), 2.17 (s, 3H, MesCH_3), 2.14 (s, 6H, MesCH_3), 2.07 (s, 3H, MesCH_3), 1.94 (br s, 6H, MesCH_3), 1.77 (m, 3H, PCHCH_3), 1.54-1.64 (m, 6H, PCHCH_3), 1.45-1.50 (m, 6H, PCHCH_3), 1.40 (dd, 3H, J = 7.1, 12.0 Hz, PCHCH_3), 1.28 (dd, 6H, J = 7.3, 17.7 Hz, PCHCH_3), 1.18 (dd, 3H, J = 7.1, 17.6 Hz, PCHCH_3),

0.89 (dd, 3H, J = 7.2, 17.2 Hz, PCHCH_3), 0.69-0.76 (m, 3H, PCHCH_3). 0.60-0.67 (m, 3H, PCHCH_3). $^{13}C\{^1H\}$ NMR (150 MHz, C_6D_6): δ 148.73 (s, C≡C), 148.65 (s, MesAr), 148.43 (s, MesAr), 148.33 (s, MesAr), 148.20 (s, MesAr), 148.10 (s, C≡C) 138.88 (s, MesAr), 133.98 (s, Ph), 133.59 (MesAr), 132.89 (s, Ph), 131.40 (s, MesAr), 131.31 (s, MesAr), 130.72 (s, MesAr), 130.40 (s, MesAr), 130.12 (s, C=C), 129.05 (s, MesAr), 128.96 (s, MesAr), 128.21 (s. Ph), 126.94 (s. Ph), 126.40 (s. Ph), 125.85 (s. Ph), 125.40 (s, C=C), 124.54 (s. Ph), 38.56 (br m, PCHCH$_3$), 36.99 (br m, PCHCH$_3$), 34.74 (br m, PCHCH$_3$), 34.10 (br m, PCHCH$_3$), 28.40 (d, J = 9.5 Hz, PCHCH$_3$), 27.94 (d, J = 9.5 Hz, PCHCH$_3$), 24.48 (MesCH$_3$), 23.14 (d, J = 11.3 Hz, PCHCH$_3$), 22.71 (MesCH$_3$), 22.67 (MesCH$_3$), 22.50 (m, PCHCH$_3$), 22.23 (d, J = 7.7 Hz, PCHCH$_3$), 21.45 (MesCH$_3$), 20.97 (MesCH$_3$), 20.45, 20.39, 20.33, 20.30, 20.26 (MesCH$_3$), 20.18 (overlapping, PCHCH$_3$), 20.14 (overlapping, PCHCH$_3$), 20.09 (overlapping, PCHCH$_3$), 19.75 (d, J =10.5 Hz, PCHCH$_3$), 18.85 (d, J = 3.0 Hz, PCHCH$_3$), 18.57 (d, J = 3.0 Hz, PCHCH$_3$). $^{31}P\{^1H\}$ NMR (161.8 MHz, C_6D_6): δ 51.81 (br overlapping s, 1P), 51.45 (br overlapping s, 1P), 24.92 (s, 1P). Satisfactory elemental analysis and/or HRMS data could not be obtained for complex **2** owing to the thermal and air/moisture sensitivity of the complex. Anal. Calcd for $C_{61}H_{87}N_3P_3CoZr$: C, 66.26; H, 7.93; N 3.80. Found: C, 65.64; H, 7.99; N, 3.79.

Synthesis of **3**

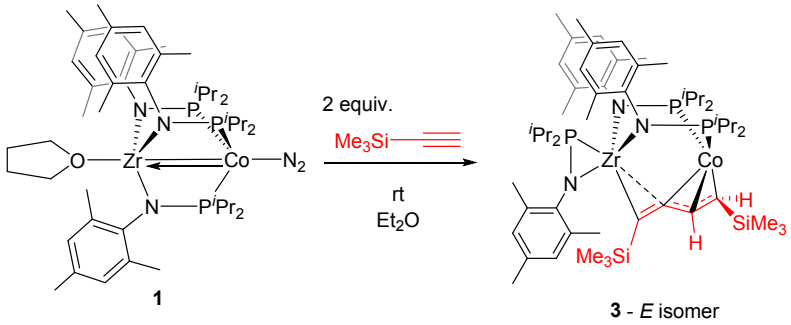

Using a micropipetter, trimethylsilylacetylene (6.8 µL, 0.048 mmol) was added to a stirring solution of complex **1** (23.8 mg, 0.0228 mmol) dissolved in Et_2O (4 mL) at room temperature. The reaction mixture was allowed to stir for 30 minutes, then filtered through a pad of Celite. The solvent was removed from the filtrate *in vacuo*, affording **3** as an analytically pure brown solid (23.3 mg, 89.5 % yield). ^1H NMR (400 MHz, C_6D_6): δ 7.68 (d, 1H, J = 19.0 Hz, CH), 6.80 (s, 4H, Mes), 6.66 (s, 2H, Mes), 5.84 (d, 1H, J = 18.9 Hz, CH), 3.73 (septet, 1H, J = 7.7 Hz, PCHCH$_3$), 3.62 (septet, 1H, J = 8.3 Hz, PCHCH$_3$), 2.93-3.09 (overlapping septets, 2H, PCHCH$_3$), 2.68 (br,

3H, MesCH$_3$), 2.57 (br s, 6H, MesCH$_3$), 2.15 (s, 12H , MesCH$_3$), 2.05 (s, 6H, MesCH$_3$), 1.86 (septet, 2H, J = 7.3 Hz, PC*H*CH$_3$), 1.68-1.74 (m, 6H, PCHC*H*$_3$), 1.59-1.65 (m, 6H, PCHC*H*$_3$) 1.45-1.54 (overlapping m, 6H, PCHC*H*$_3$), 1.34 (dd, 3H, J = 7.3, 18.3 Hz, PCHC*H*$_3$), 1.22 (dd, 3H, J = 7.4, 17.6 Hz, PCHC*H*$_3$), 0.75 (dd, 3H, J = 7.1, 11.5 Hz, PCHC*H*$_3$), 0.63-0.71 (overlapping m, 9H, PCHC*H*$_3$), 0.42 (s, 9H, Si(C*H*$_3$)$_3$), 0.29 (s, 9H, Si(C*H*$_3$)$_3$). ^{13}C{^{1}H} NMR (150 MHz, C_6D_6): δ 149.13 (s, C≡C), 149.04 (s, MesAr), 148.97 (s, MesAr), 148.89 (s, MesAr), 148.79 (s, MesAr), 148.69 (s, C≡C), 145.23 (s, C=C), 133.89 (s, MesAr), 133.77 (s, MesAr), 131.67 (s, MesAr), 131.57 (s, MesAr), 131.50 (s, MesAr), 131.07 (s, MesAr), 129.51 (s, MesAr), 128.59 (s, MesAr), 126.76 (s, C=C), 38.82 (d, J = 10.4 Hz, P*C*HCH$_3$), 37.63 (br m, P*C*HCH$_3$), 35.83 (d, J = 10.0 Hz, P*C*HCH$_3$), 30.24 (d, J = 9.7 Hz, P*C*HCH$_3$), 29.81 (d, J = 13.1 Hz, P*C*HCH$_3$), 23.87 (d, J = 8.8 Hz, PCH*C*H$_3$), 23.57 (d, J = 8.6 Hz, PCH*C*H$_3$), 23.00 (d, J = 10.5 Hz, PCH*C*H$_3$), 22.66 (d, J = 10.5 Hz, PCH*C*H$_3$), 22.29 (Mes*C*H$_3$), 22.08 (Mes*C*H$_3$), 21.95 (d, J = 7.5 Hz, PCH*C*H$_3$), 21.15 (Mes*C*H$_3$), 21.04 (d, J = 6.0 Hz, PCH*C*H$_3$), 20.94 (d, J = 7.5 Hz, PCH*C*H$_3$), 20.83 (Mes*C*H$_3$), 20.73 (d, J = 7.5 Hz, PCH*C*H$_3$), 20.68 (Mes*C*H$_3$), 19.50 (d, J = 19.5 Hz, PCH*C*H$_3$), 2.09 (s, Si*C*H$_3$), -0.76 (s, Si*C*H$_3$). ^{31}P{^{1}H} NMR (161.8 MHz, C_6D_6): δ 50.18 (br s, 1P), 47.86 (br s, 1P), 21.73 (s, 1P). Anal. Calcd for $C_{55}H_{95}N_3P_3Si_2CoZr$: C, 60.18; H, 8.72; N, 3.83. Found: C 59.93; H, 8.80; N, 3.88.

Synthesis of **5**

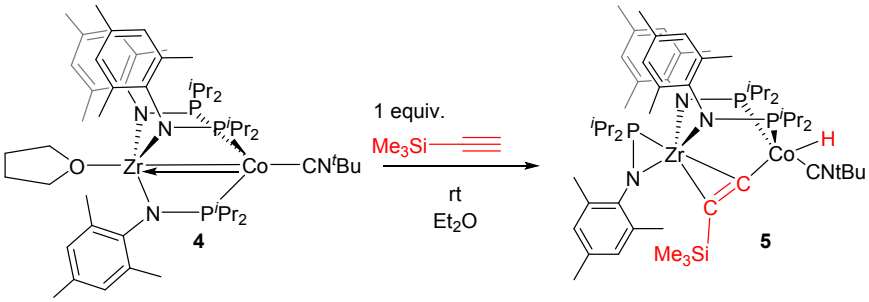

Using a micropipetter, trimethylsilylacetylene (3.3 µL, 0.024 mmol) was added to a stirring solution of **4** (24.9 mg, 0.0235 mmol) in Et$_2$O (4 mL) at room temperature. The reaction mixture was allowed to stir for one hour. The resulting solution was filtered through a pad of Celite and the solvent was removed from the filtrate *in vacuo* to afford **5** in spectroscopically pure form (15.6 mg, 57.4% yield). X-ray quality crystals were grown from a concentrated solution of **5** in Et$_2$O stored at -35 °C for 48 hours. ^{1}H NMR (400 MHz, C_6D_6): δ 6.86 (s, 2H, MesH), 6.80 (s,

4H, MesH), 3.17 (br, 2H, PC*H*CH_3), 2.78 (s, 6H, MesCH_3), 2.65 (s, 6H, MesCH_3), 2.41 (br, 2H, PC*H*CH_3), 2.31 (s, 6H, MesCH_3), 2.18 (s, 6H, MesCH_3), 2.13 (s, 3H, MesCH_3), 1.89 (m 6H, PCHC*H*$_3$), 1.53 (m, 6H, PCHC*H*$_3$), 1.25 (m, 6H, PCHC*H*$_3$), 1.18 (br, 2H, PC*H*CH_3), 1.07 (s, 9H, CN^{t}Bu), 0.93 (m, 6H, PCHC*H*$_3$), 0.85 (m, 6H, PCHC*H*$_3$), 0.72 (dd, 6H, J = 7.2, 19.1 Hz, PCHC*H*$_3$), 0.14 (s, 9H, $SiMe_3$), -12.79 (t, 1H, $^2J_{H\text{-}P}$ = 56.5 Hz, Co-H). $^{13}C\{^1H\}$ NMR (150 MHz, C_6D_6): δ 151.7 (m, Co-*C*≡C), 148.18 (s, Co-C≡*C*), 135.10 (s, MesAr), 134.43 (s, MesAr), 132.70 (s, MesAr), 131.94 (s, MesAr), 131.58 (s, MesAr), 130.09 (s, MesAr), 129.81 (s, MesAr), 129.40 (s, MesAr), 54.67 (s, CN*C*$(CH_3)_3$), 34.44 (d, J = 6.0 Hz, P*C*HCH_3), 33.84 (m, two overlapping signals, P*C*HCH_3), 32.40 (s, Mes*C*H_3), 30.54 (CNC(*C*$H_3)_3$), 23.60-23.87 (m, 3 overlapping signals, PCH*C*H_3), 22.91 (s, Mes*C*H_3), 22.75 (s, Mes*C*H_3), 22.00 (d, J = 15.0 Hz, PCH*C*H_3), 21.16 (d, J = 9.0 Hz, PCH*C*H_3), 20.65 (s, Mes*C*H_3), 18.61 (d, J = 13.5 Hz, PCH*C*H_3), 2.65 (s, Si*C*H_3); *C*NtBu signal was not observed. $^{31}P\{^1H\}$ NMR (161.8 MHz, C_6D_6): δ 108.36 (br s, 2P), 8.34 (s, 1P). IR (KBr solution cell, THF): 2054 cm^{-1} (C≡N). Anal. Calcd for $C_{55}H_{94}N_4P_3SiCoZr$: C, 61.02; H, 8.75; N, 5.18; Found: C, 56.93; H, 8.36; N, 4.08. Repeated attempts to obtain satisfactory elemental analysis data resulted in consistently low %C, %H, and %N values. We tentatively attribute this to the air and moisture sensitivity of **5** and its partial decomposition during transportation/handling. For example, a sample in which all three phosphinoamide ligands were oxidized and the CN^{t}Bu ligand had dissociated (i.e. $C_{57}H_{85}N_3P_3O_3SiCoZr$) and evaporated would have C, 57.34; H, 8.18; N, 4.01.

<u>Reaction of **1** with 1 equivalent of trimethylsilylacetylene</u>

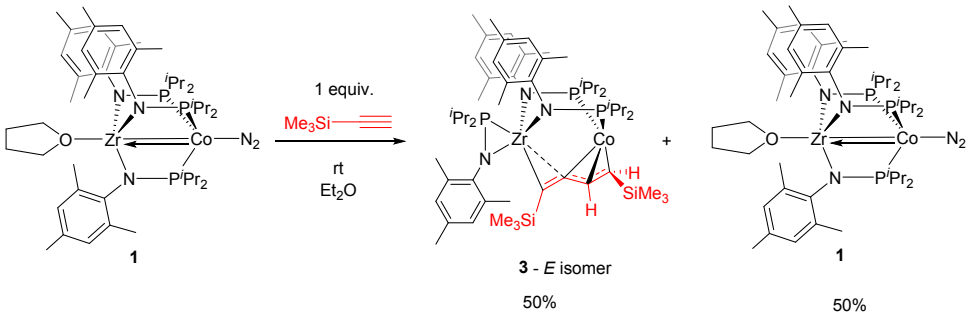

Using a micropipetter, trimethylsilylacetylene (4.0 µL, 0.028 mmol) was added to a stirring solution of complex **1** (28.1 mg, 0.0281 mmol) dissolved in Et_2O (4 mL) at room temperature. The reaction mixture was allowed to stir for 30 minutes, then filtered through a pad of Celite. The

solvent was removed from the filtrate *in vacuo*. Analysis of the reaction mixture by $^{31}P\{^{1}H\}$ NMR spectroscopy showed an approximately 50:50 mixture of **1** and **3** (see Figure S24).

Reaction of **1** with excess phenylacetylene

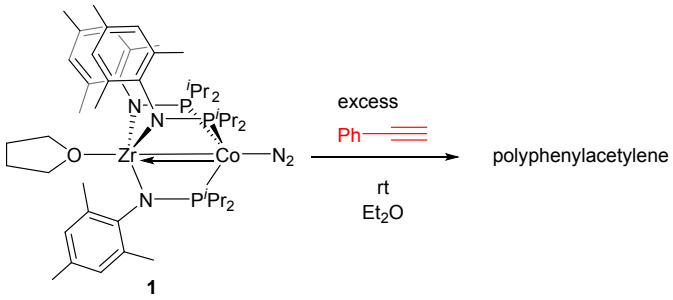

To a stirring solution of **1** (22.4 mg, 0.0224 mmol) in C_6H_6 (0.8 mL) was added phenylacetylene (200 µl, 1.82 mmol). The reaction mixture was allowed to stir for 16 hours, at which time hexanes (10 mL) was added, resulting in formation of an orange solid. The red supernatant was decanted from the solid. The solid was then washed with an additional 10 mL of hexanes and dried *in vacuo* (33.6 mg). The orange solid was confirmed to be polyphenylacetylene by ^{1}H NMR and FT-IR spectroscopy (See Figures S25 and S26).[5, 6] GC-MS analysis of the reaction mixture showed no evidence for the formation of cyclotrimerization products (see Figure S27).

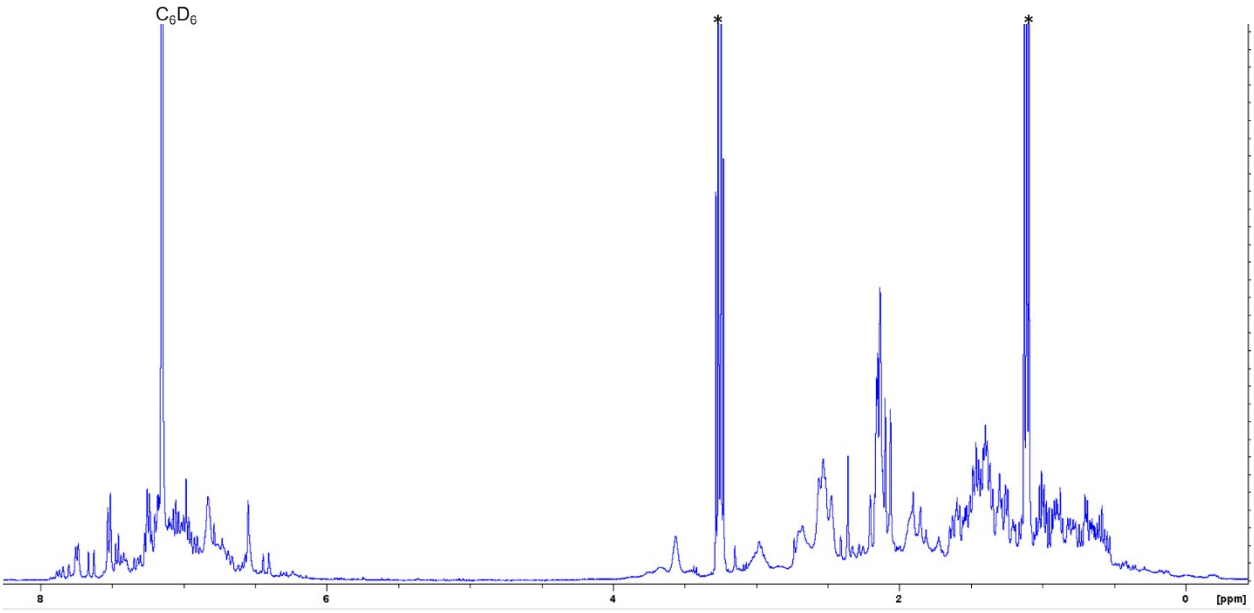

Figure S1. ^{1}H NMR (400 MHz, C_6D_6) spectrum of the reaction of PhCCH and **1** at room temperature in C_6D_6. Residual THF peaks are labeled with a *.

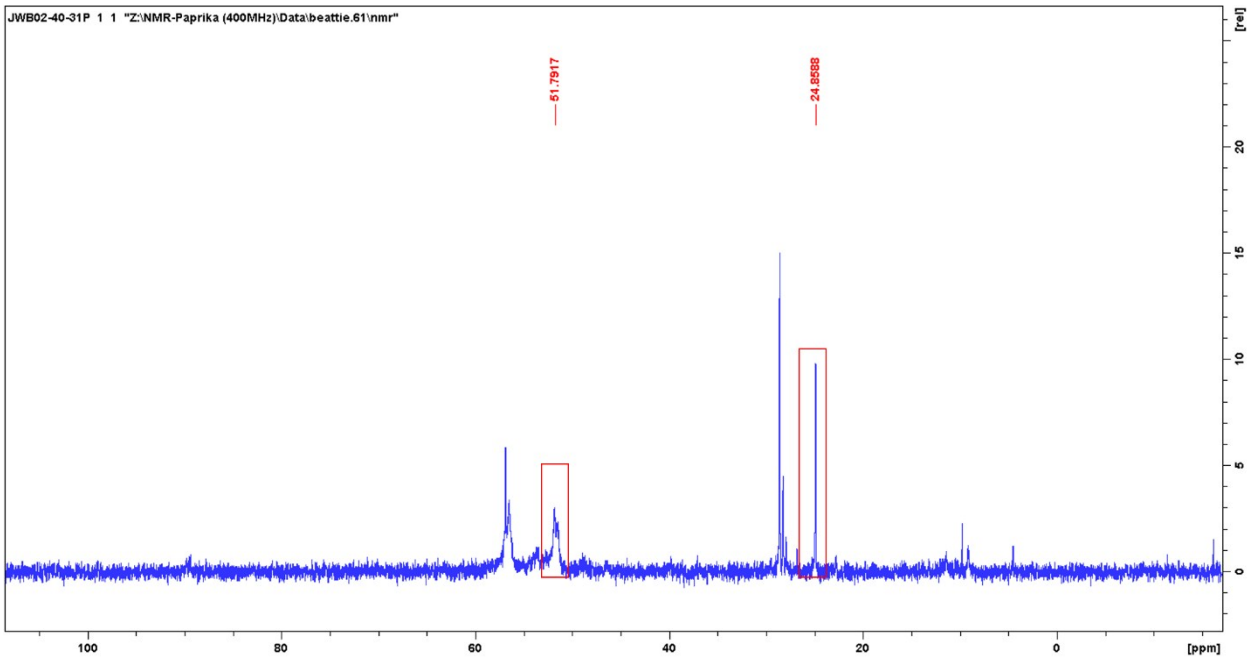

Figure S2. $^{31}P\{^{1}H\}$ NMR (161.8 MHz, C_6D_6) spectrum of the reaction of PhCCH and **1** at room temperature. Resonances in red boxes correspond to **2b**.

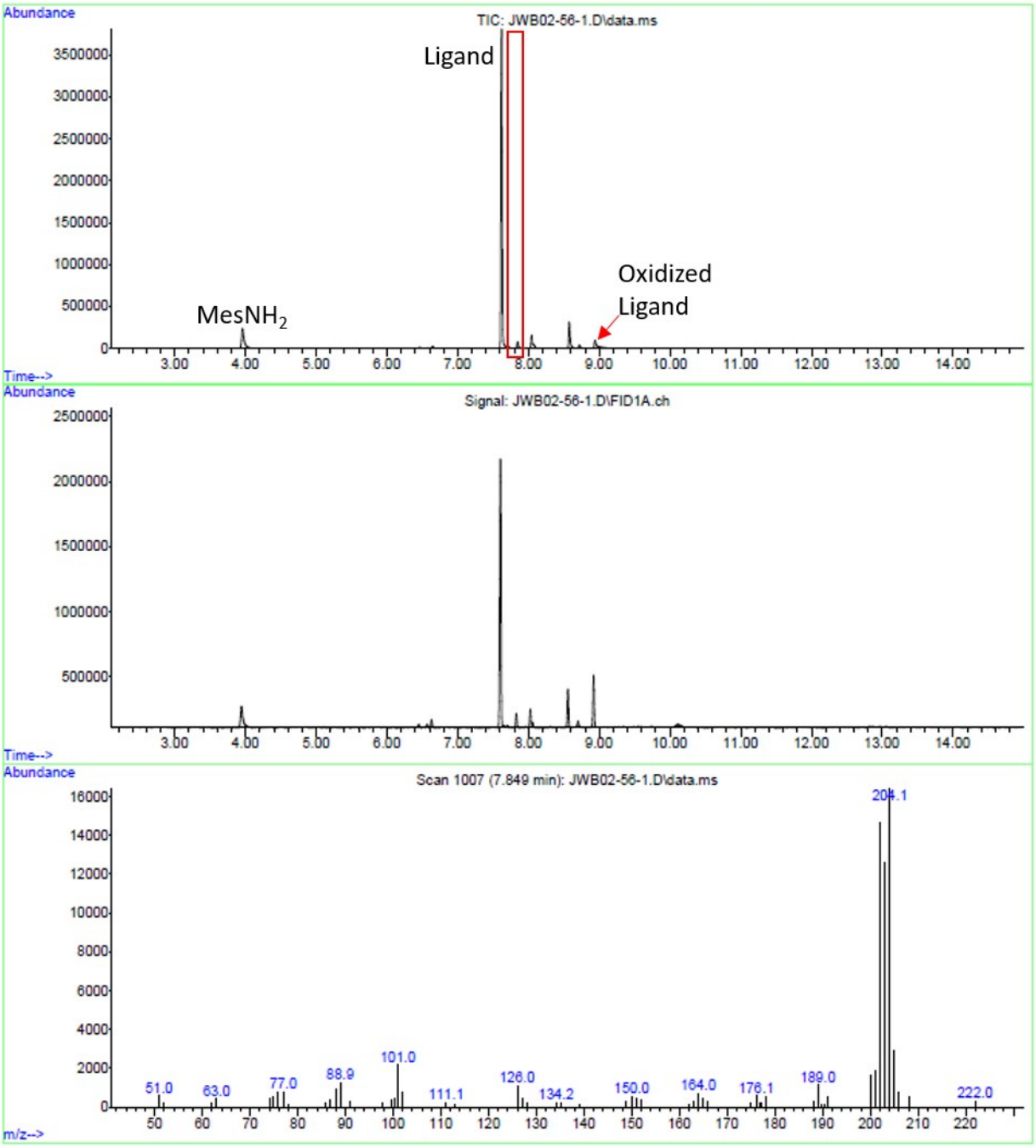

Figure S3. GC-MS-FID of the reaction of **1** with phenylacetylene at room temperature showing the mass spectrum of the peak at 7.849 min (red box) which corresponds to the *gem* isomer.

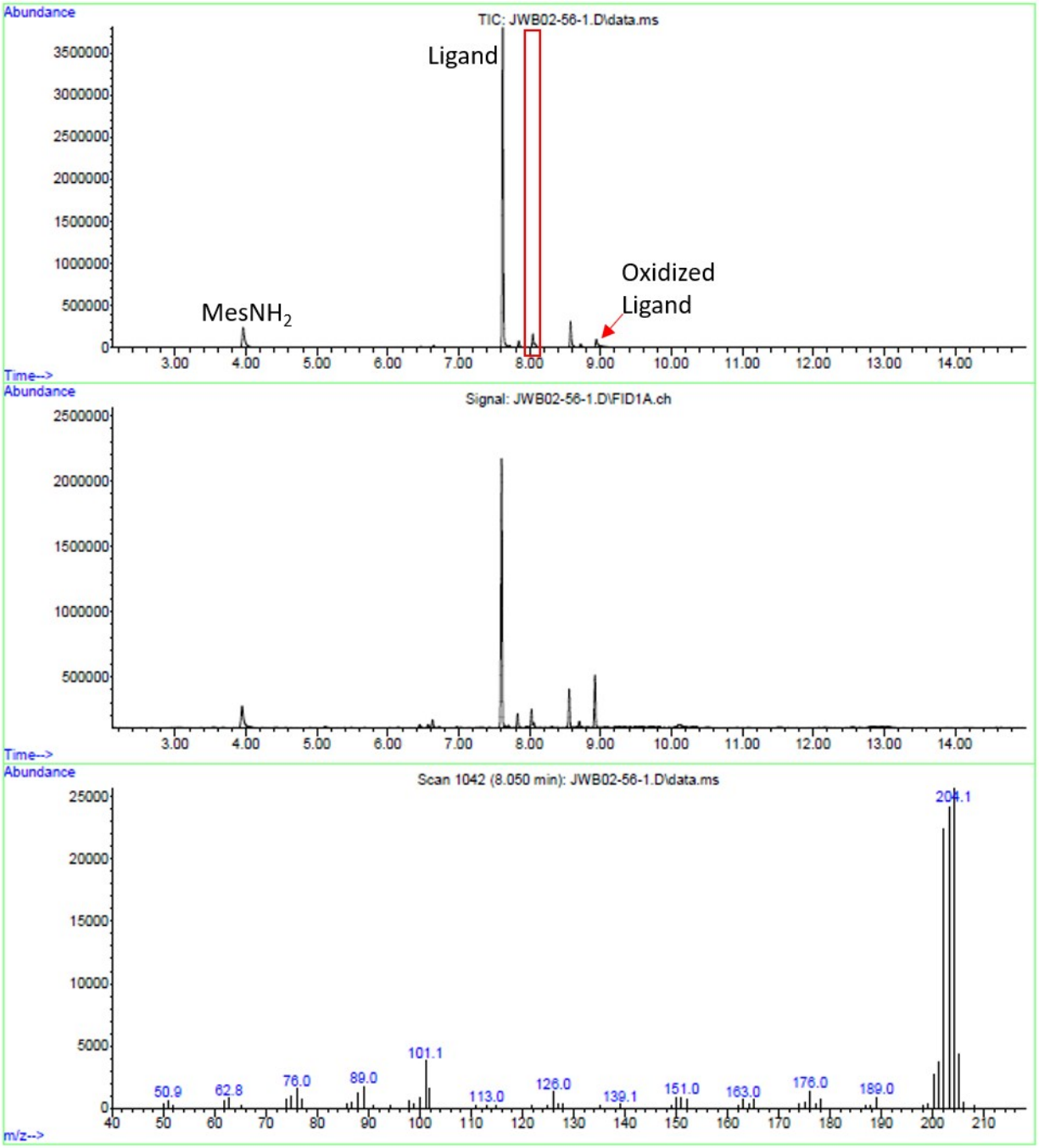

Figure S4. GC-MS-FID of the reaction of **1** with phenylacetylene at room temperature showing the mass spectrum of the peak at 8.050 min (red box) corresponding to the *Z* isomer.

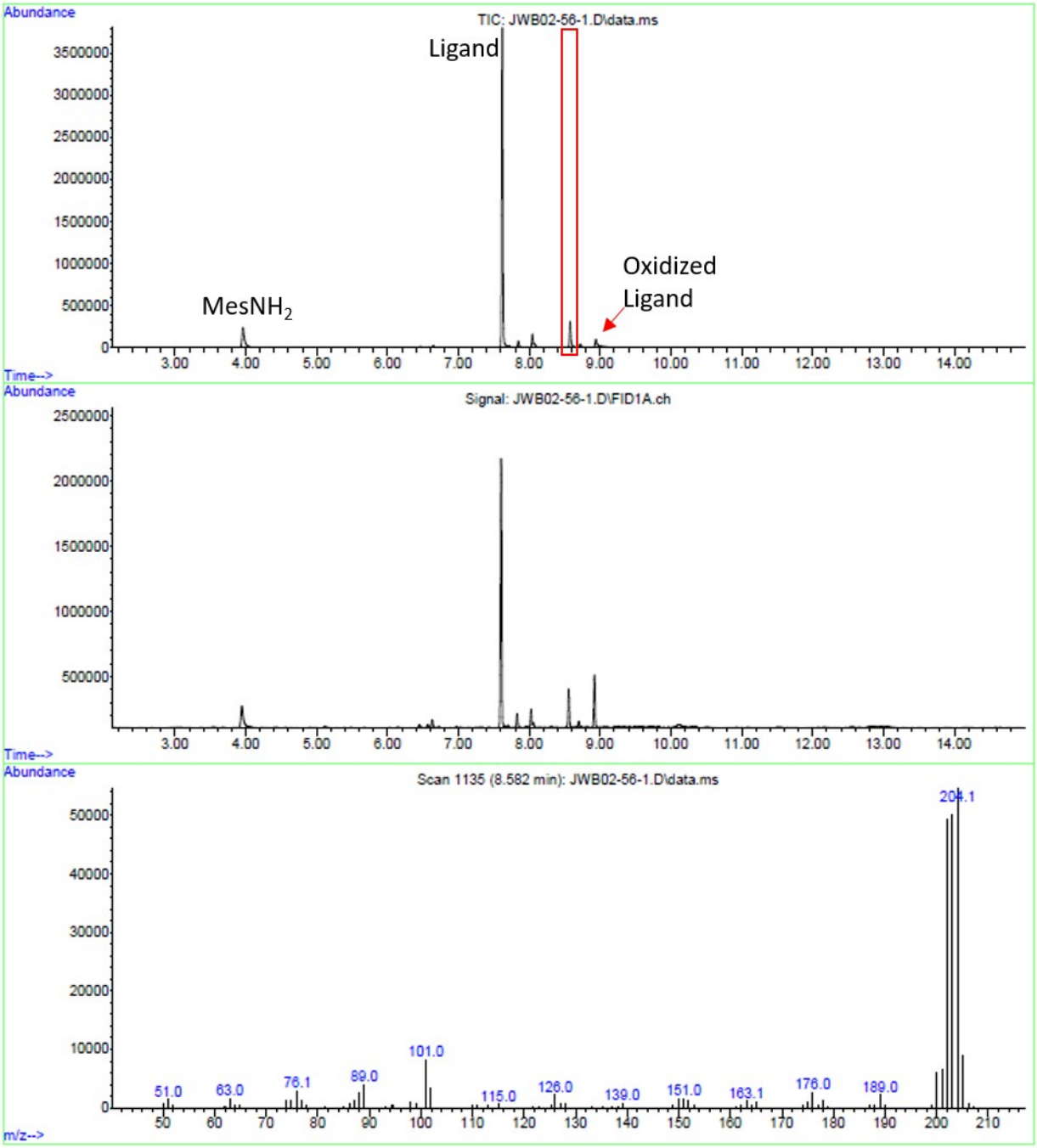

Figure S5. GC-MS-FID of the reaction of **1** with phenylacetylene at room temperature showing the mass spectrum of the peak at 8.582 min (red box) corresponding to the *E* isomer.

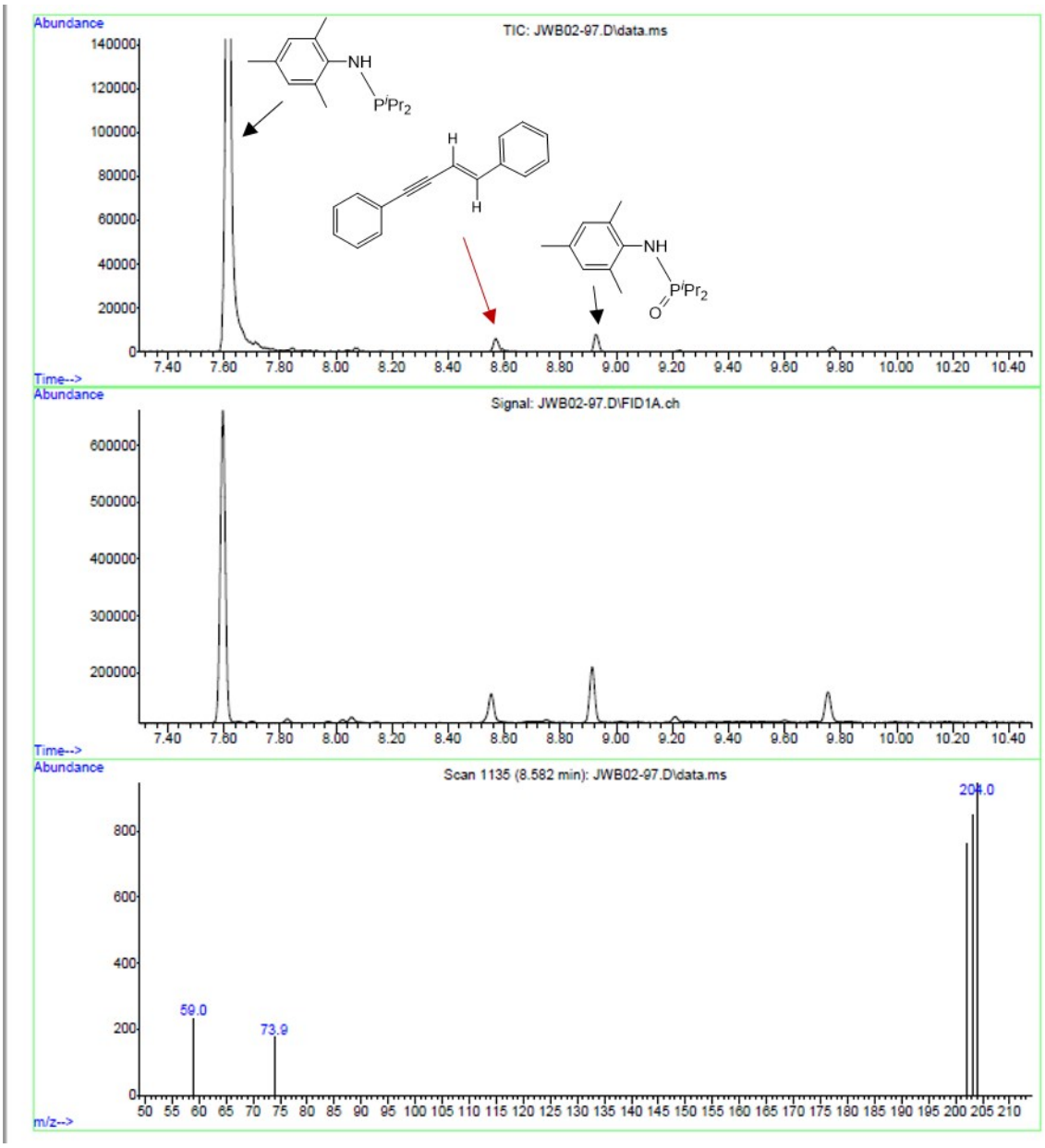

Figure S6. GC-MS-FID of the reaction of **1** with phenylacetylene at low temperature showing the mass spectrum of the peak at 8.582 min corresponding to the *E* isomer.

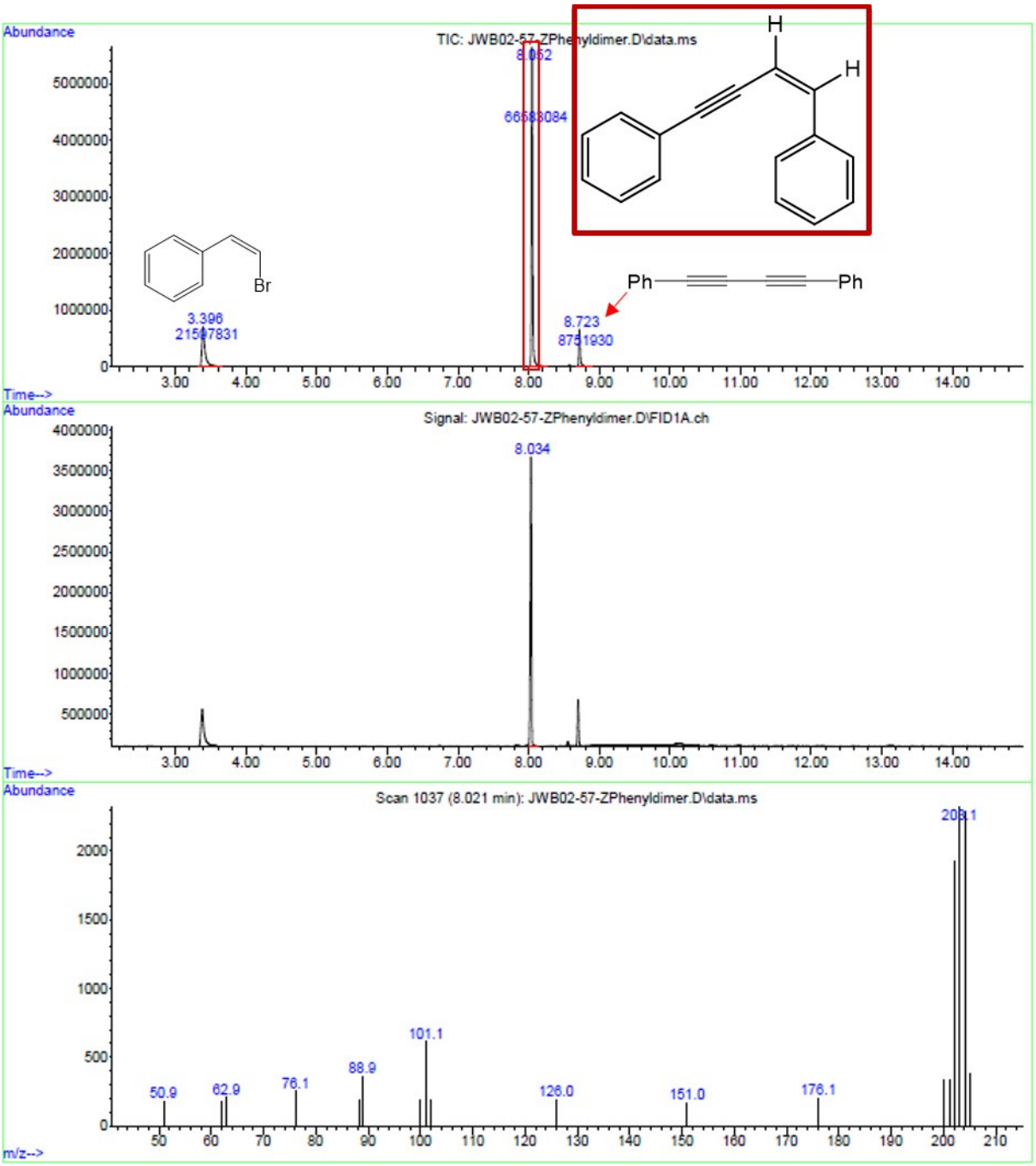

Figure S7. GC-MS-FID of the reaction of the independently synthesized *Z*-1,3-enyne, showing the mass spectrum corresponding to the peak at 8.034 min.

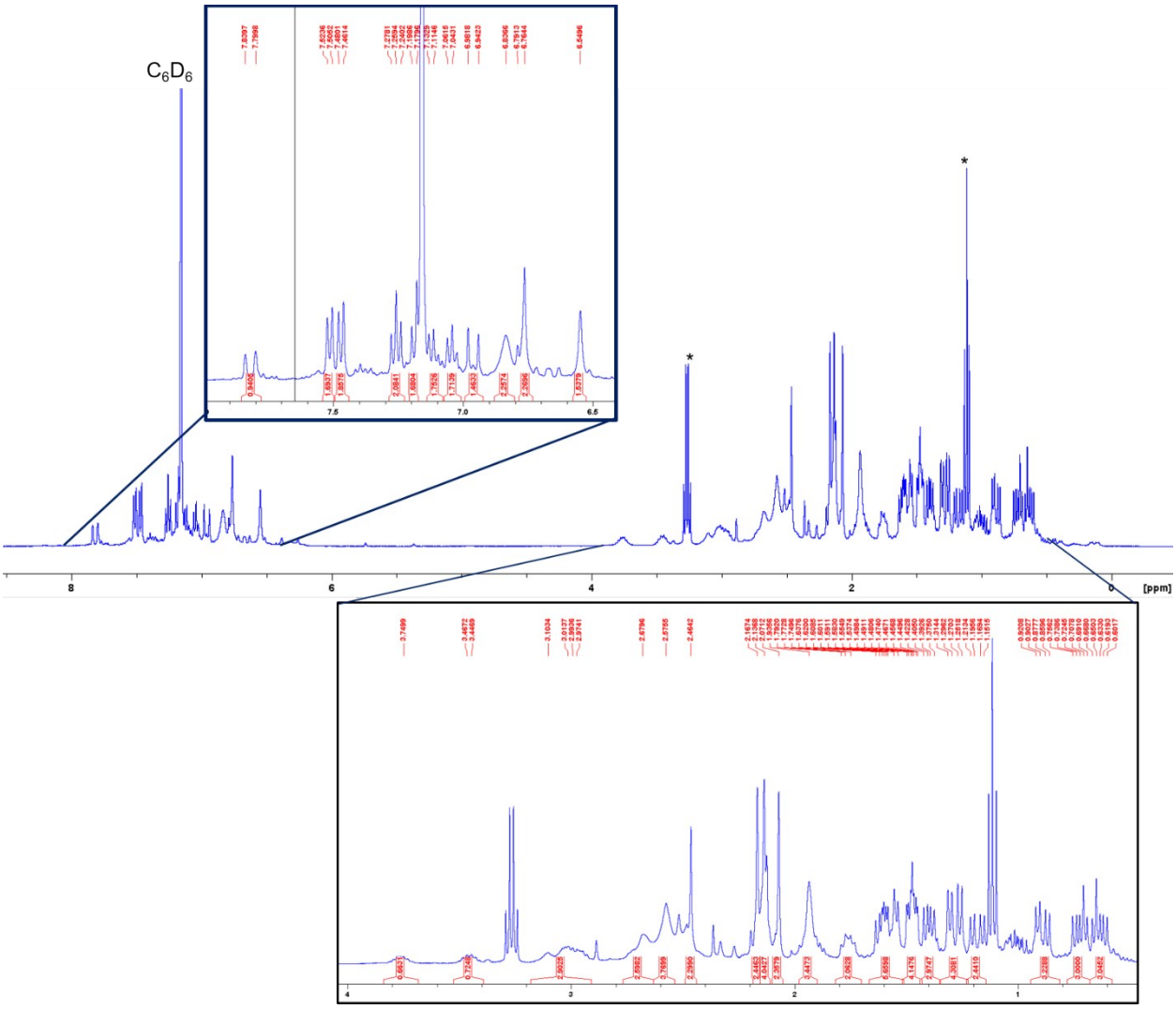

Figure S8. ^{1}H NMR (400 MHz, C_6D_6) spectrum of **2b**. Residual solvent peaks from Et_2O are labeled with *.

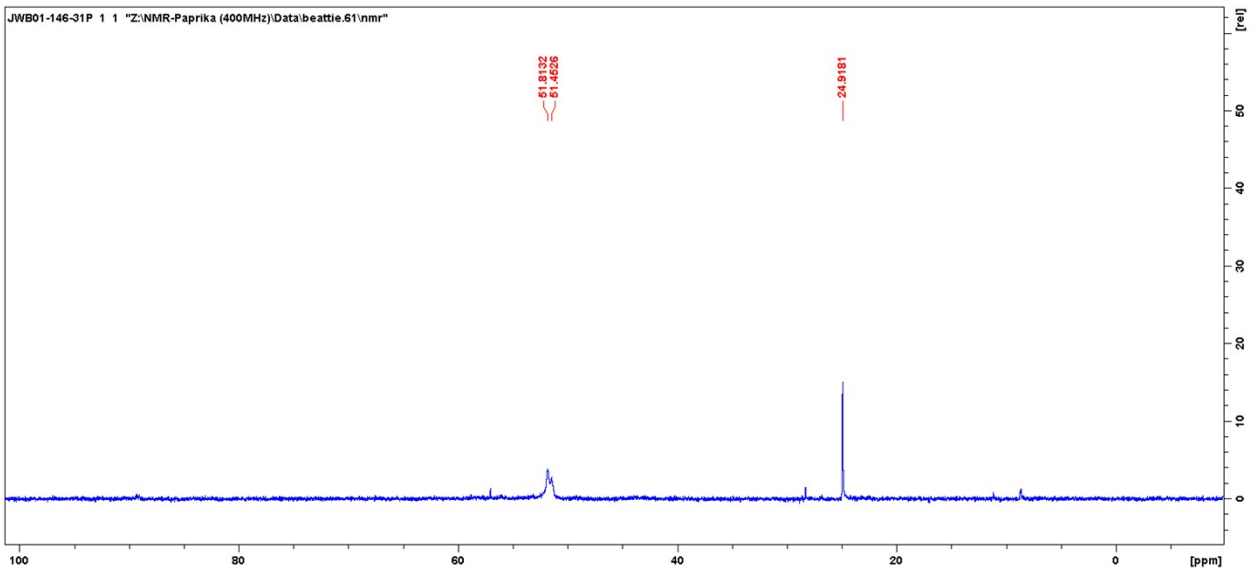

Figure S9. $^{31}P\{^{1}H\}$ NMR (161.8 MHz, C_6D_6) spectrum of **2b**.

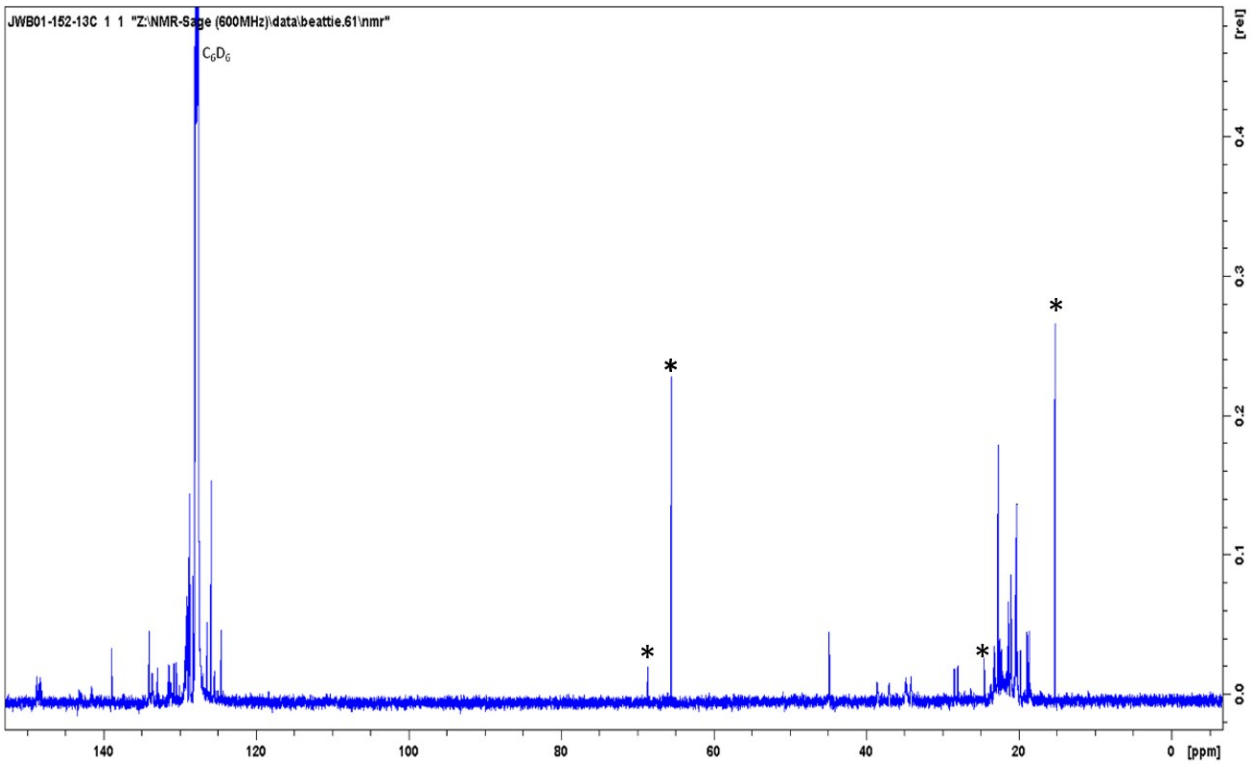

Figure S10. $^{13}C\{^{1}H\}$ NMR (150 MHz, C_6D_6) spectrum of **2b**. Residual Et_2O and THF peaks are labeled with a *.

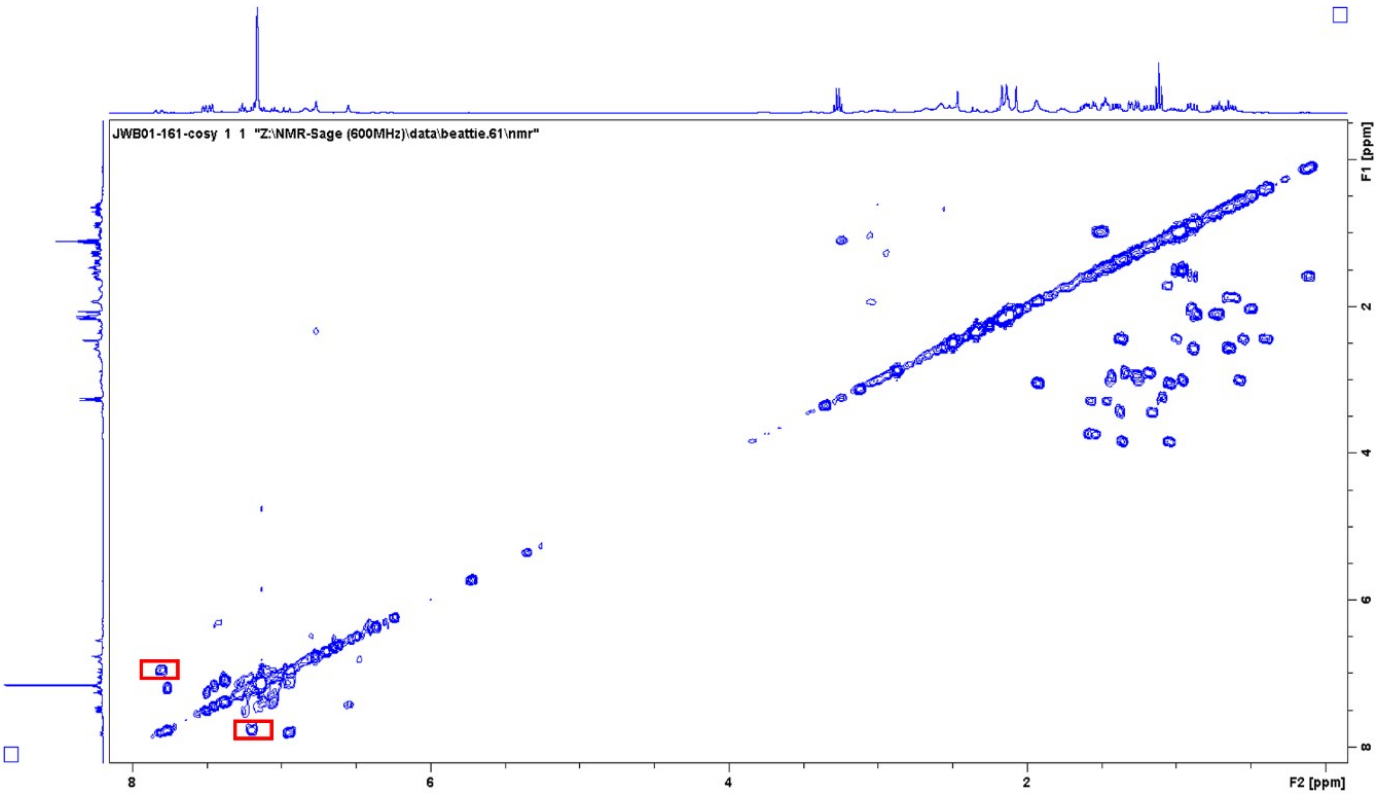

Figure S11. ^{1}H – ^{1}H COSY (600 MHz, C_6D_6) spectrum of **2b** with red boxes to indicate alkene cross peaks.

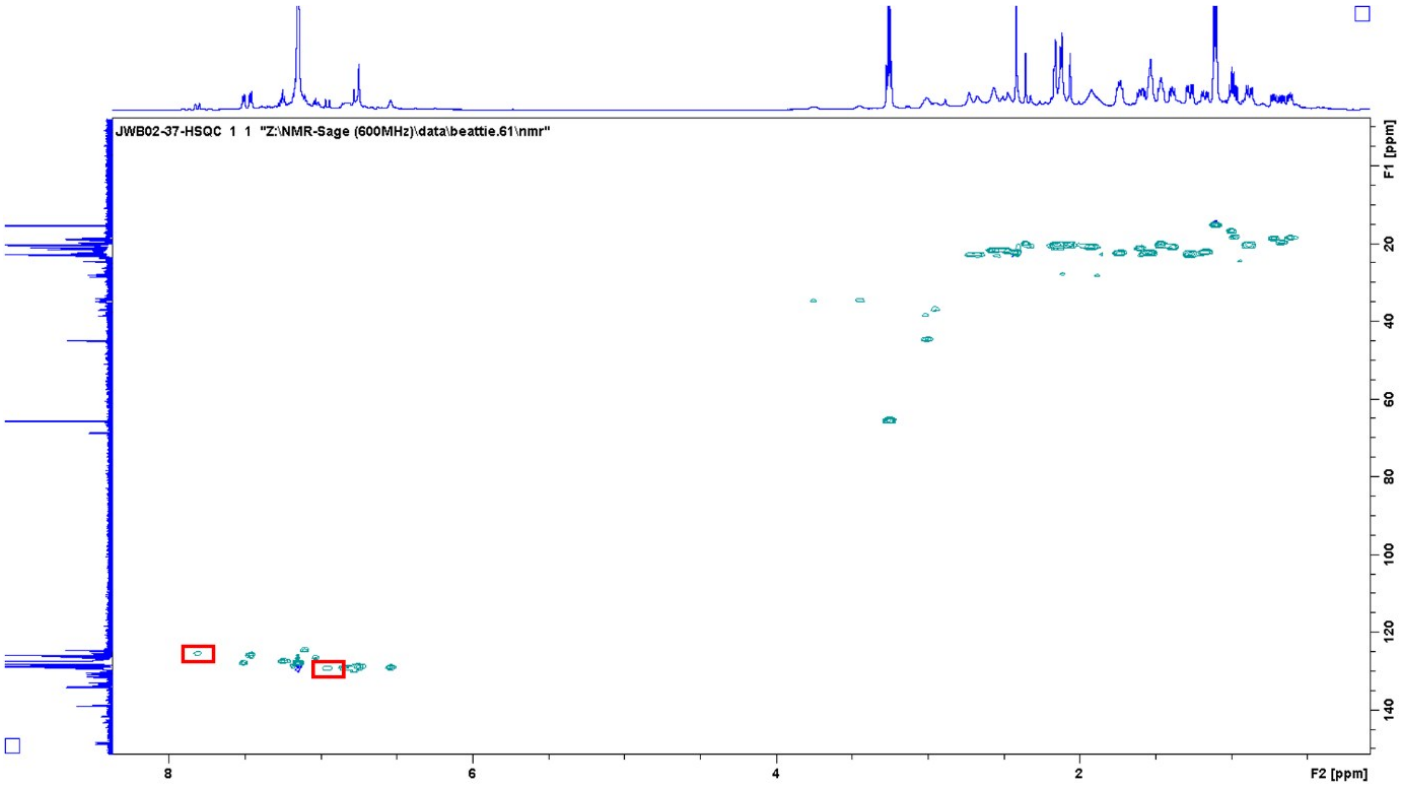

Figure S12. ^{1}H – ^{13}C HSQC (600 MHz, C_6D_6) spectrum of **2b** with red boxes to indicate alkene cross peaks.

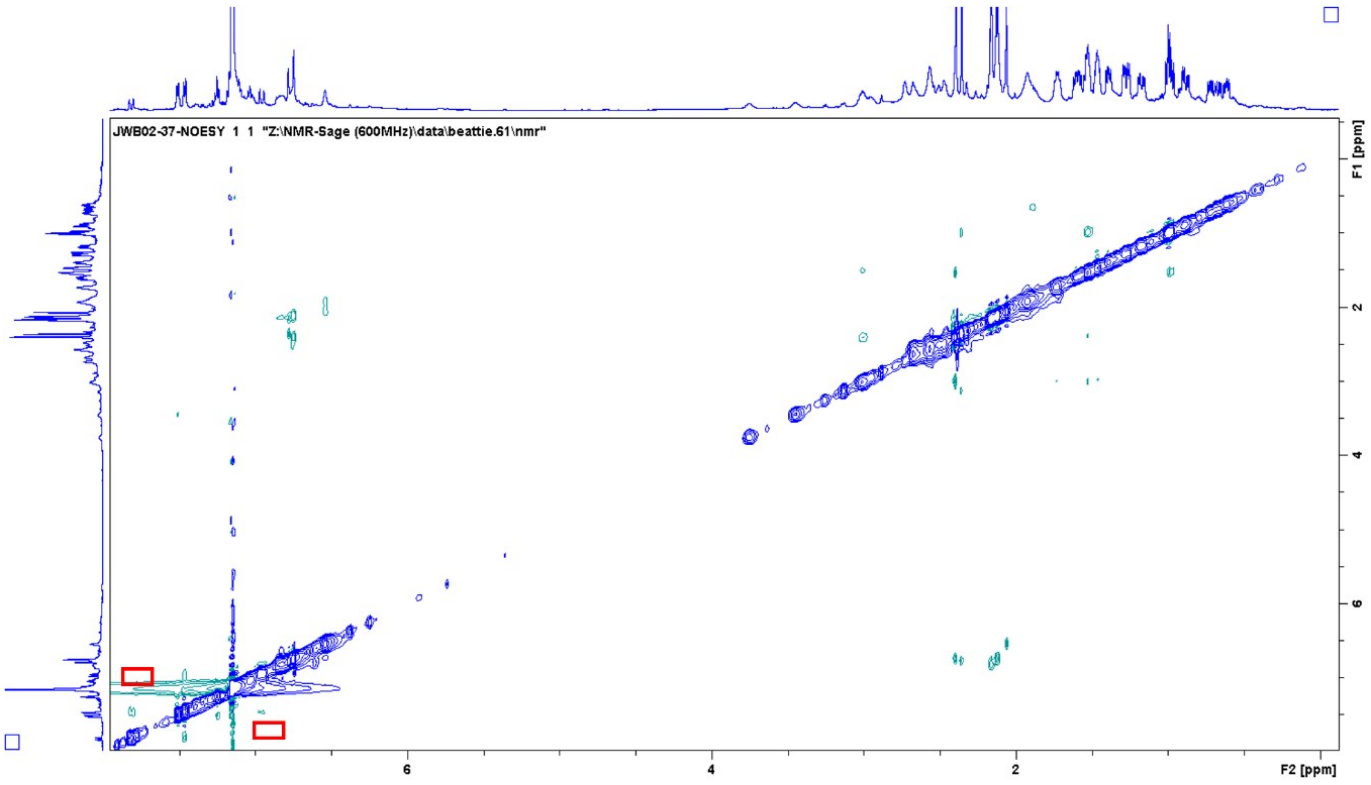

Figure S13. $^{1}H - {}^{1}H$ NOESY (600 MHz, C_6D_6) spectrum of **2b** with red boxes to indicate area of possible alkene cross peaks.

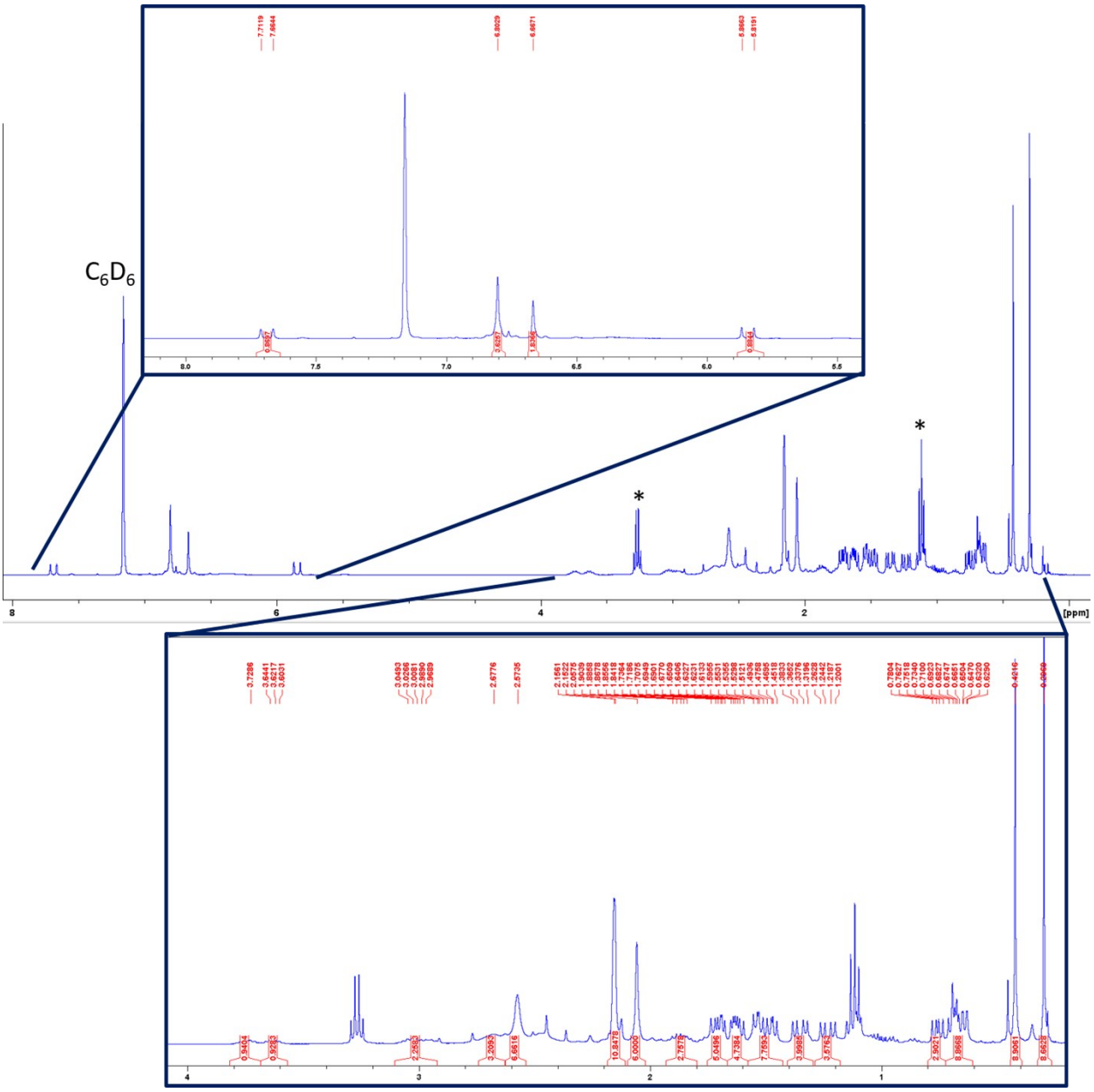

Figure S14. ^{1}H NMR (400 MHz, C_6D_6) spectrum of **3**. Residual Et_2O solvent peaks are labeled with a *.

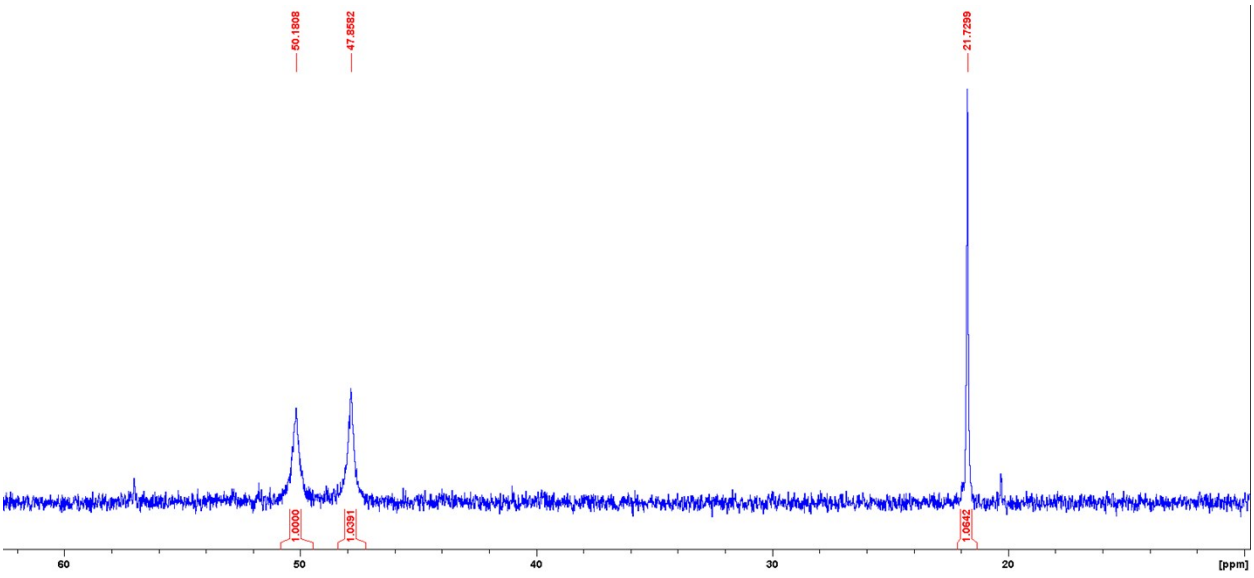

Figure S15. $^{31}P\{^{1}H\}$ NMR (161.8 MHz, C_6D_6) spectrum of **3**.

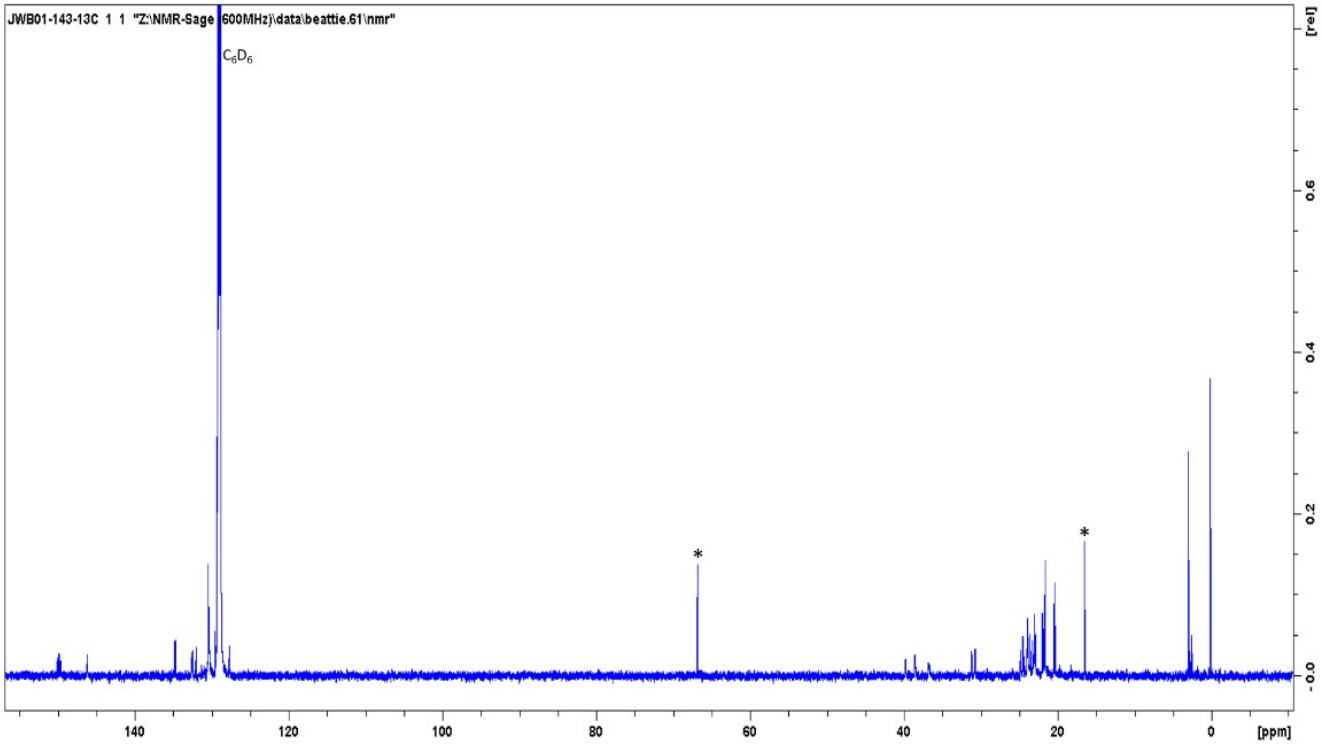

Figure S16. $^{13}C\{^{1}H\}$ NMR (150 MHz, C_6D_6) spectrum of **3**. Residual Et_2O solvent peaks are Et_2O labeled with a *.

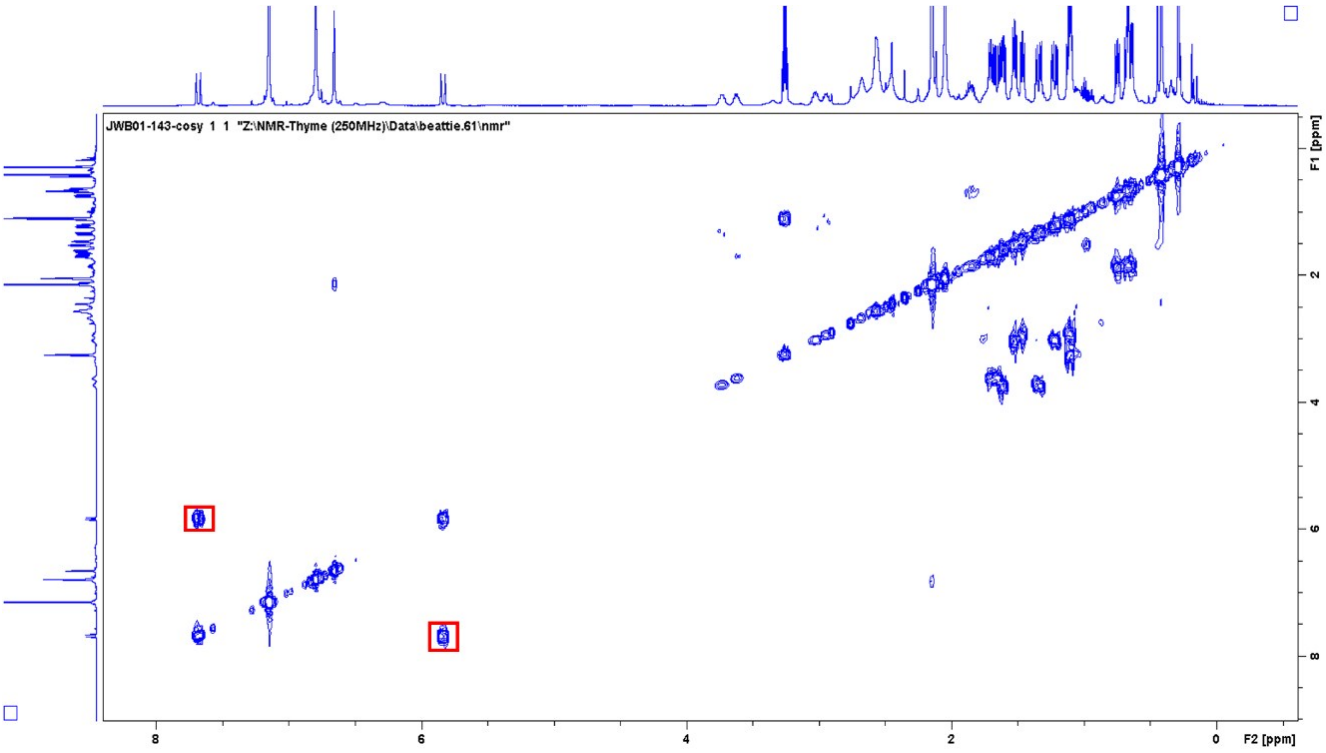

Figure S17. ^{1}H – ^{1}H COSY spectrum (250 MHz, C_6D_6) of **3** with red boxes to indicate alkene cross peaks.

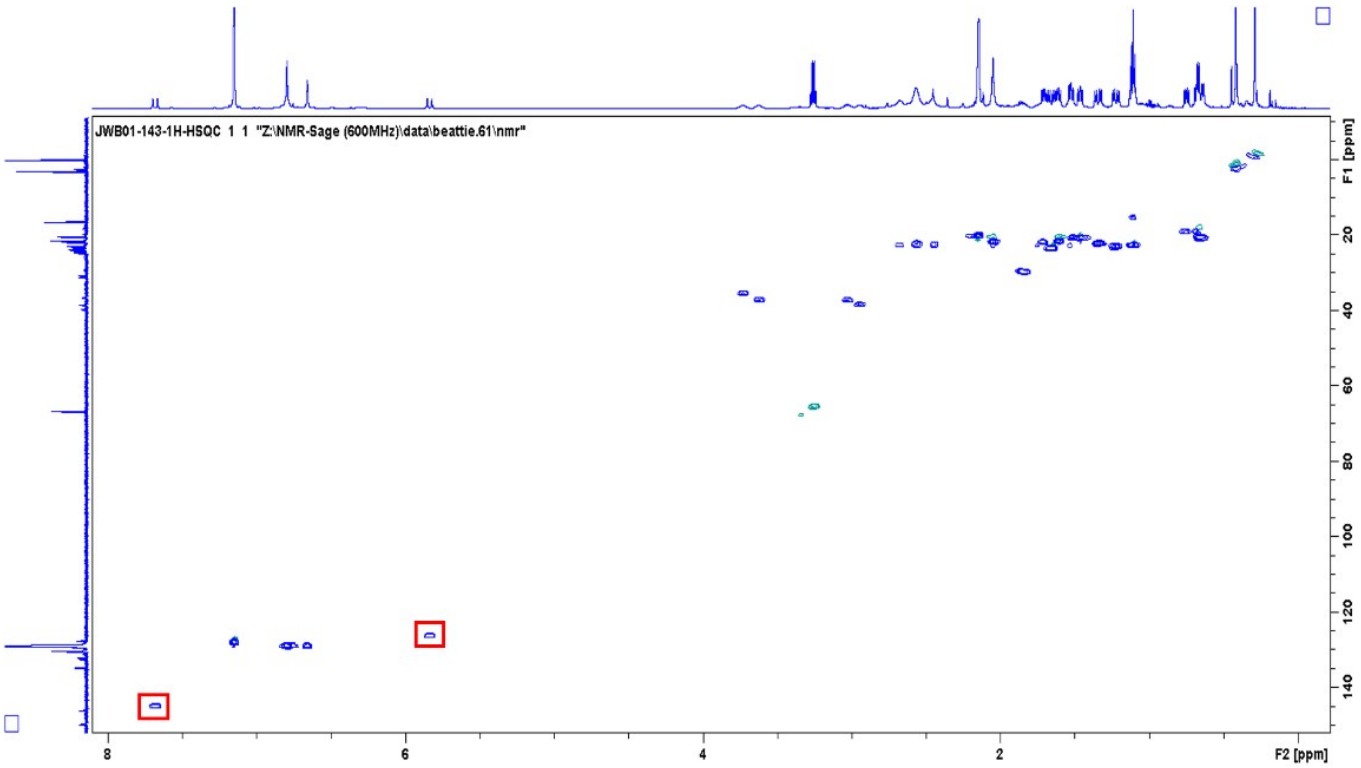

Figure S18. ^{1}H – ^{13}C HSQC (600 MHz, C_6D_6) spectrum of **3** with red boxes to indicate alkene cross peaks.

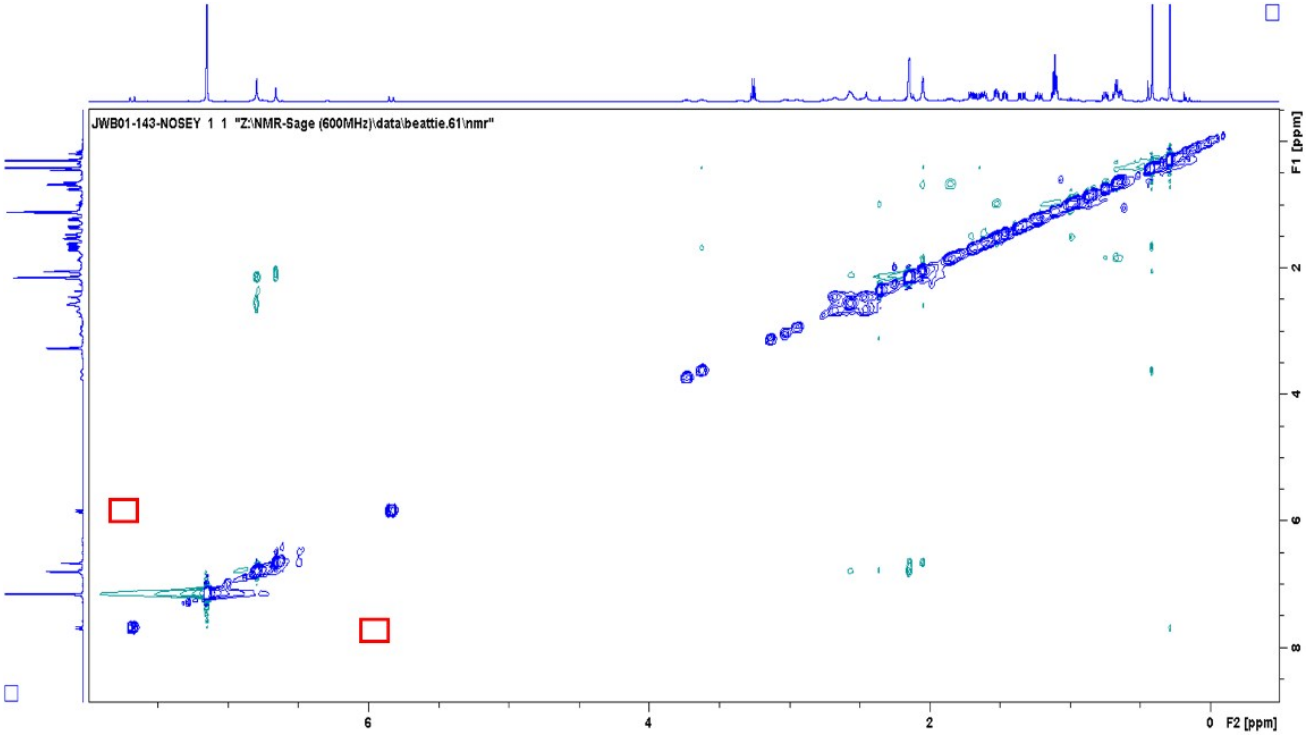

Figure S19. ^{1}H – ^{1}H NOESY spectrum (600 MHz, C_6D_6) of **3** with red boxes to indicate area of possible alkene cross peaks.

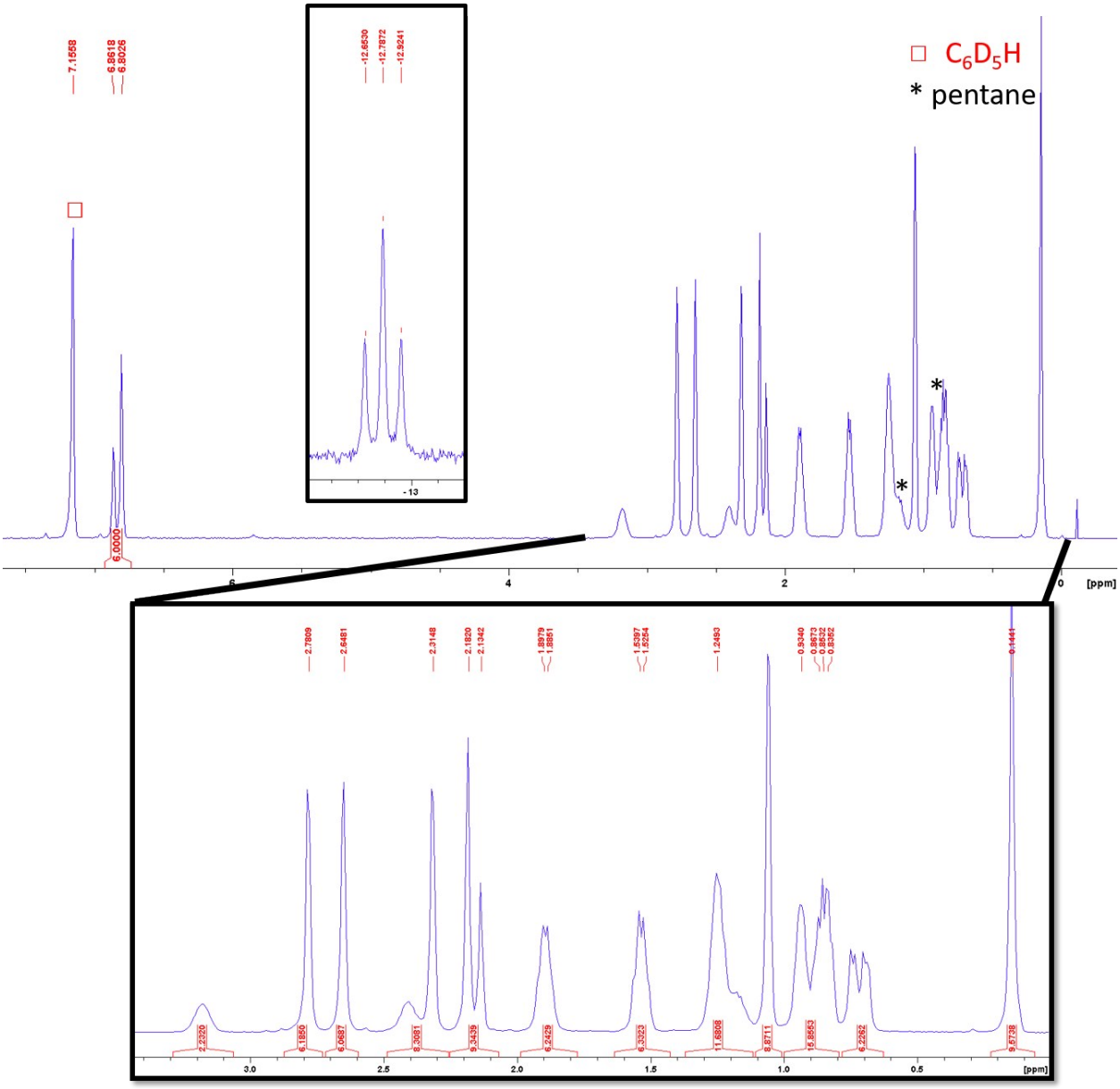

Figure S20. ^{1}H NMR spectrum (400 MHz, C_6D_6) of **5** with inset showing Co-hydride signal. Residual pentane signals (marked with a *) overlap with signals from **5** leading to higher integrations than expected.

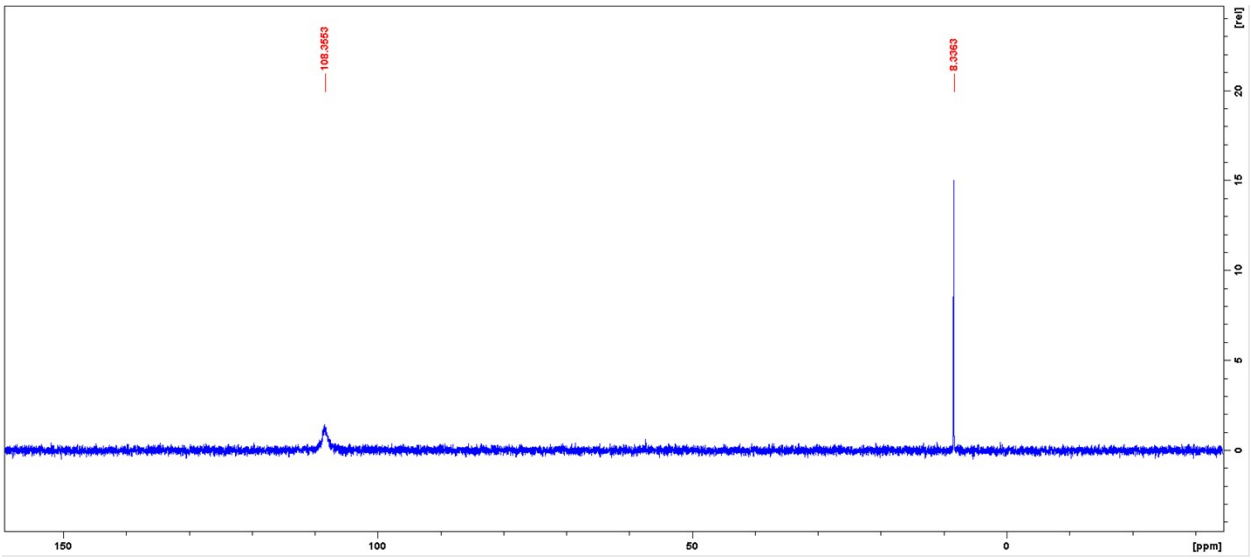

Figure S21. $^{31}P\{^{1}H\}$ NMR (161.8 MHz, C_6D_6) spectrum of **5**.

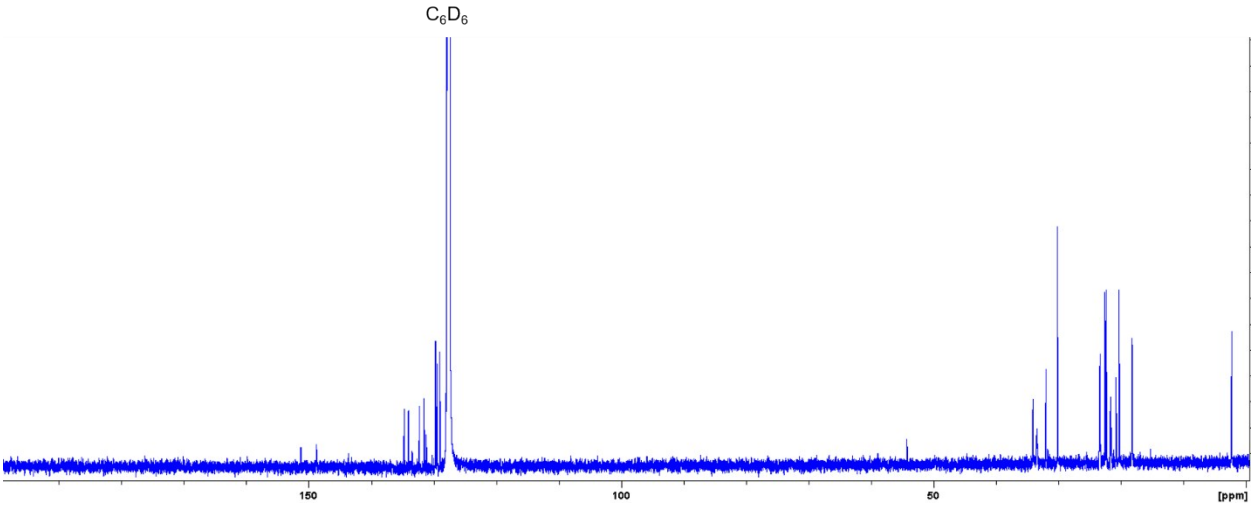

Figure S22. $^{13}C\{^{1}H\}$ NMR (150 MHz, C_6D_6) spectrum of **5**.

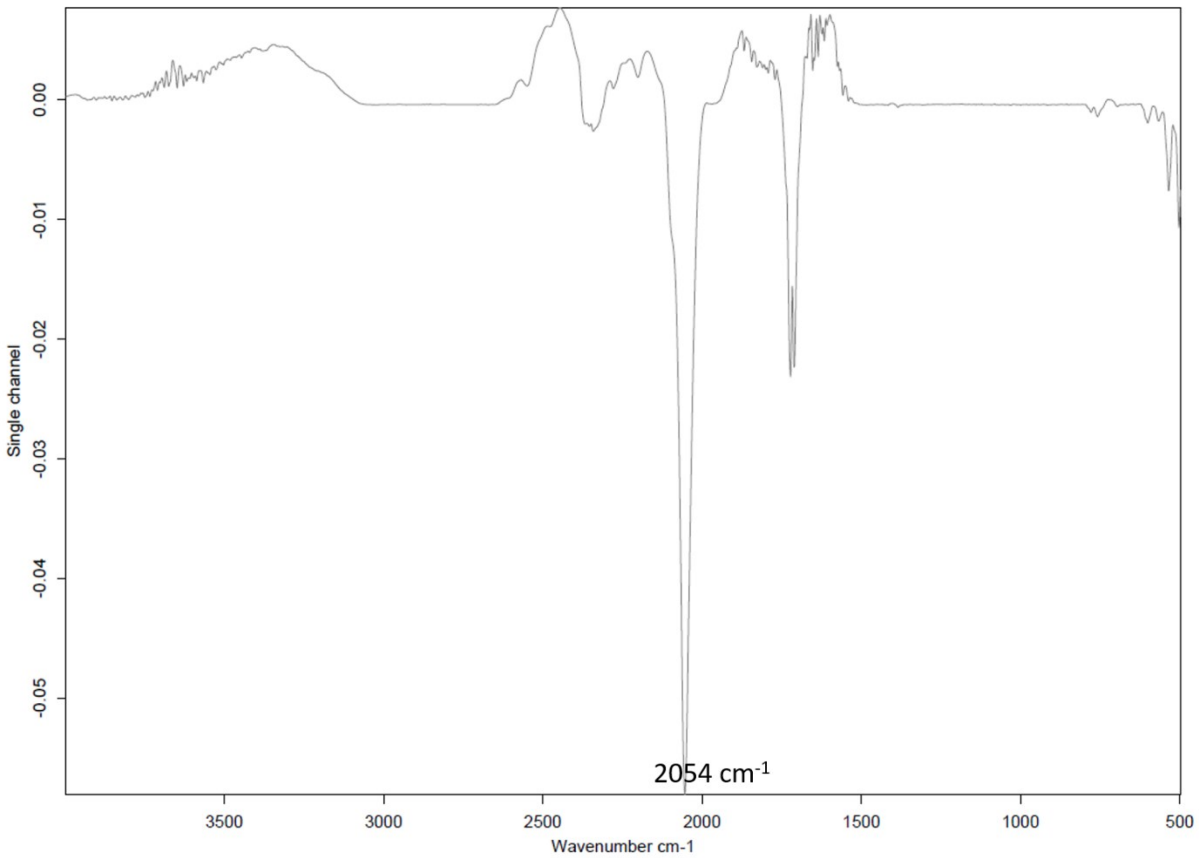

Figure S23. IR spectrum (KBr solution cell, THF) of **5** with C≡N stretch labeled.

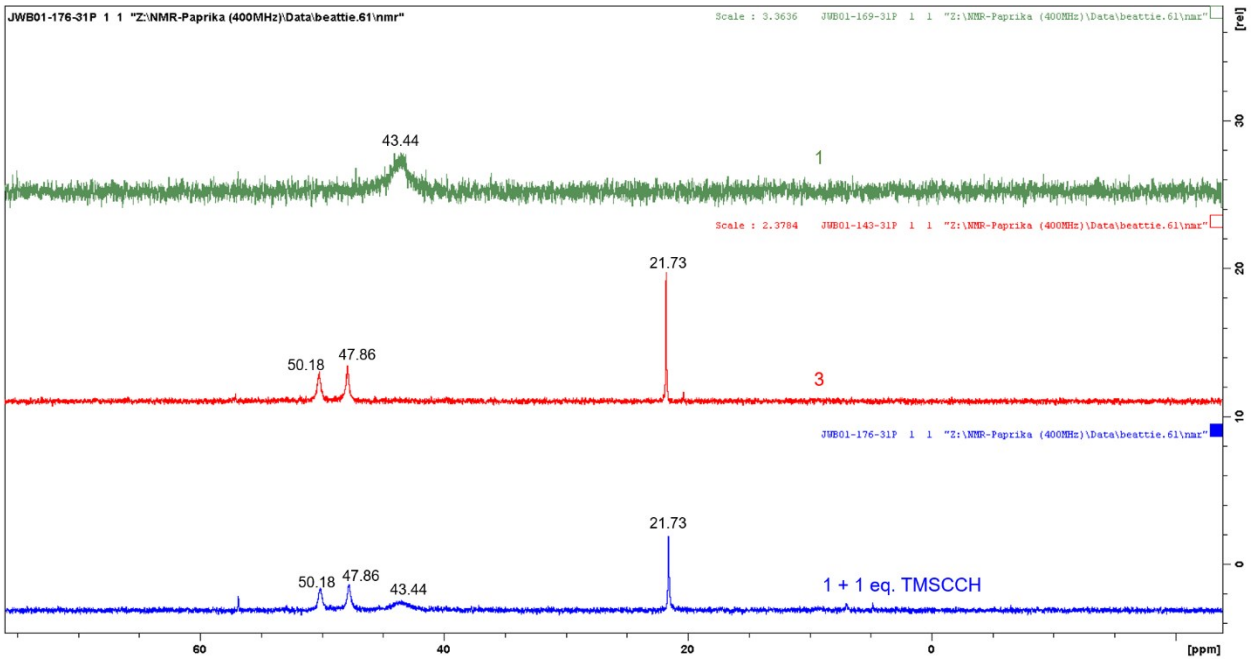

Figure S24. Bottom: $^{31}P\{^{1}H\}$ NMR spectrum of the reaction of **1** with one equivalent of TMSCCH. Middle: $^{31}P\{^{1}H\}$ NMR of **3**. Top: $^{31}P\{^{1}H\}$ NMR spectrum of **1**.

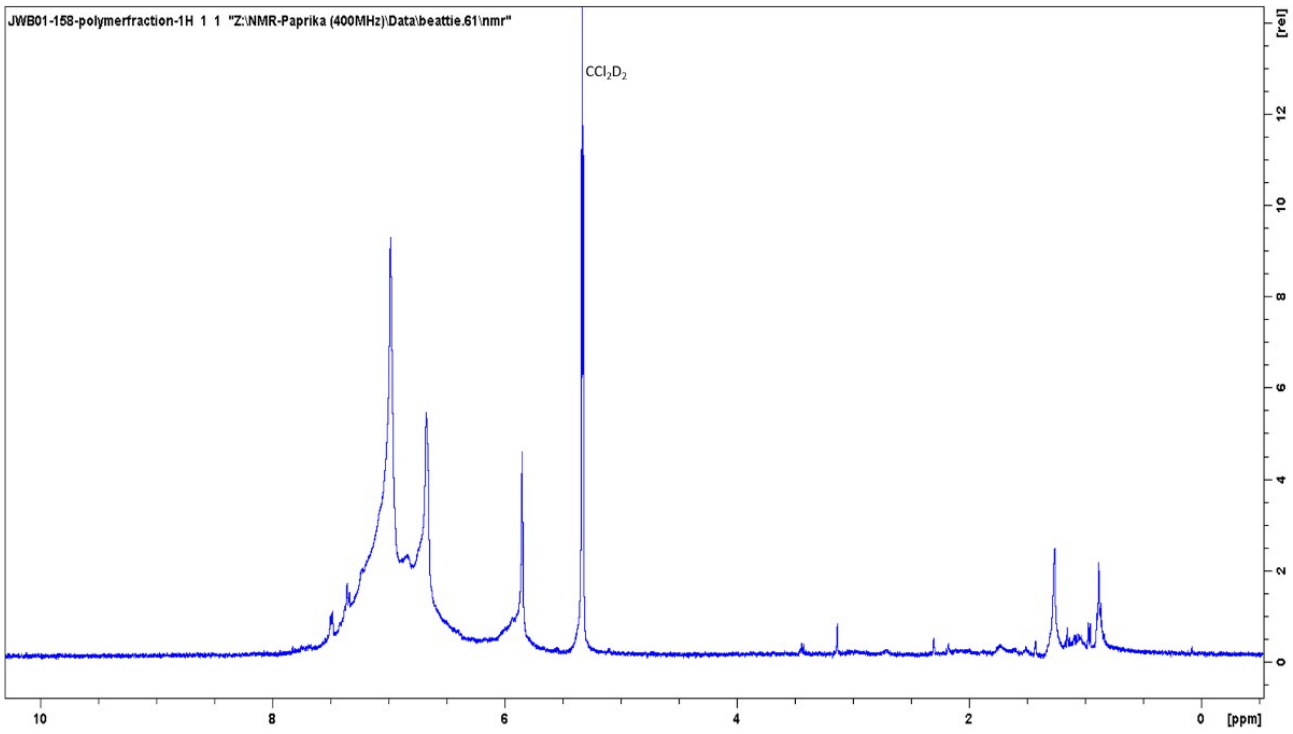

Figure S25. ^{1}H NMR spectrum (400 MHz, CD_2Cl_2) of extracted polymer from the reaction of **1** with excess PhCCH.

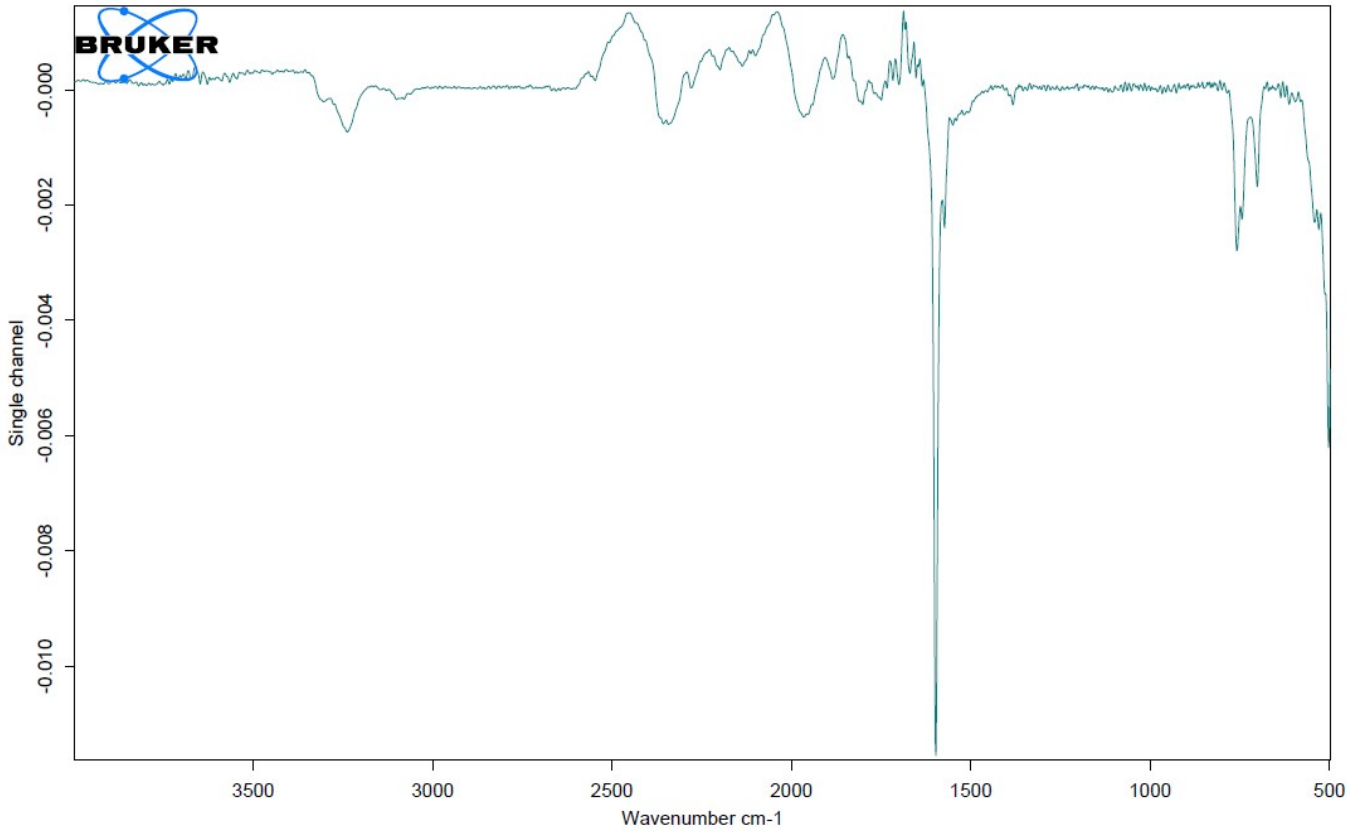

Figure S26. IR spectrum (KBr solution cell, CH_2Cl_2) of polyphenylacetylene formed in the reaction of **1** with excess PhCCH.

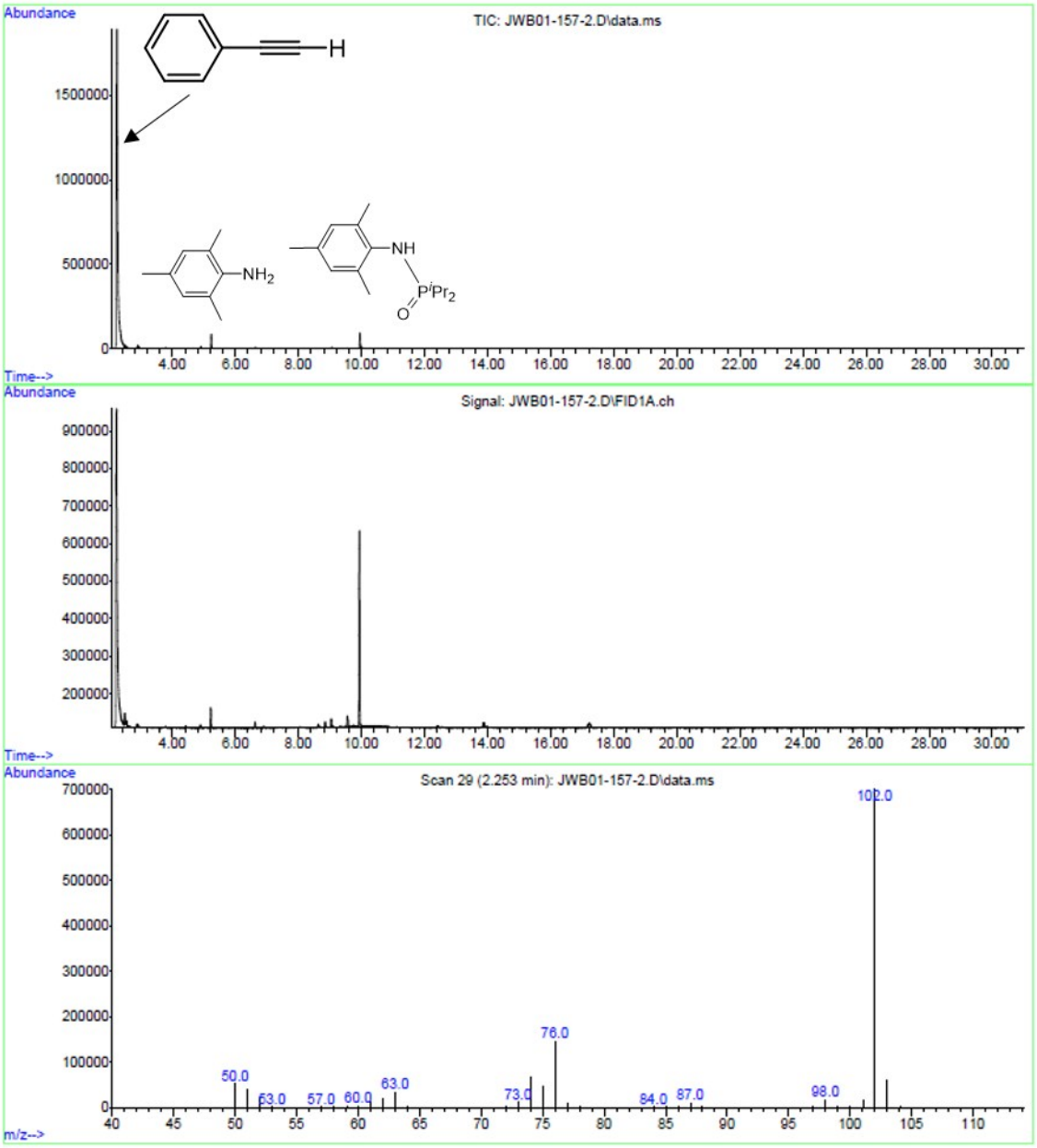

Figure S27. GC-MS-FID of the reaction of **1** with excess phenylacetylene at room temperature, confirming that no cyclotrimerization or dimerization products were formed under these conditions.

Table S1. X-Ray Crystallographic Data.

	2a	**5**
CCDC number	1965575	1965048
Empirical formula	$C_{61}H_{87}CoN_3P_3Zr$	$C_{55}H_{94}CoN_4P_3SiZr$
Formula weight (g/mol)	1105.46	1082.49
Temperature (K)	120	100
λ (Å)	0.71073	0.71073
Crystal system	Monoclinic	monoclinic
Space group	$P2_1/n$	C2/c
a (Å)	12.0196(9)	49.022(4)
b (Å)	34.104(3)	11.4685(9)
c (Å)	13.9512(9)	25.848(3)
α (°)	90	90
β (°)	97.923(2)	120.087(5)
γ (°)	90	90
Volume (Å^3)	5664.3(7)	12574(2)
Z	4	8
ρ_{calc} (g/cm^3)	1.296	1.144
μ (mm^{-1})	0.602	0.559
Final R indexes [$I \geq 2\sigma(I)$]	$R_1 = 0.0507$, $wR_2 = 0.0731$	$R_1 = 0.1070$, $wR_2 = 0.2162$
Final R indexes [all data]	$R_1 = 0.1066$, $wR_2 = 0.0878$	$R_1 = 0.1314$, $wR_2 = 0.2274$

Figure S28. Fully labelled displacement ellipsoid (50%) of **2a**.

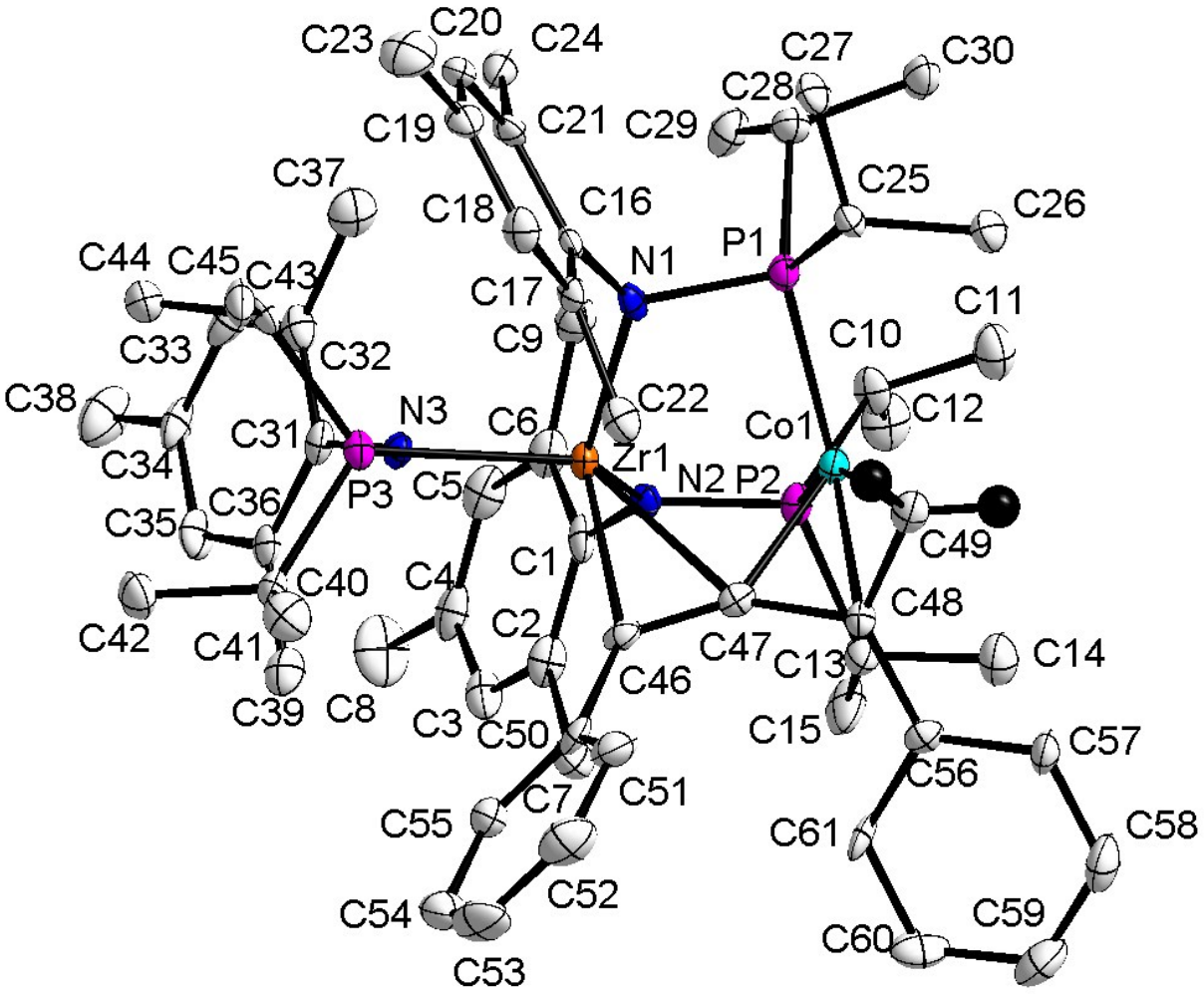

X-Ray data collection, solution, and refinement for 2a. All operations were performed on a Bruker-Nonius Kappa Apex2 diffractometer, using graphite-monochromated MoKα radiation. All diffractometer manipulations, including data collection, integration, scaling, and absorption corrections were carried out using the Bruker Apex2 software.[7] Preliminary cell constants were obtained from three sets of 12 frames. Data collection was carried out at 120 K, using a frame time of 60 sec and a detector distance of 60 mm. The optimized strategy used for data collection consisted of two phi and one omega scan sets, with 0.5° steps in phi or omega, completeness was 99.9%. A total of 1358 frames were collected. Final cell constants were obtained from the xyz centroids of 1992 reflections after integration. The largest crystal available despite many attempts of crystal growth was small in volume; and had resolution that did not exceed d= 0.91 angstroms. Accordingly, the data collection was limited to a maximum two-theta value of ca. 46 degrees.

From the systematic absences, the observed metric constants and intensity statistics, space group $P2_1/n$ was chosen initially, subsequent solution and refinement confirmed the correctness of this choice. The structure was solved using *SIR-92*,[8] and refined (full-matrix-least squares) using the Oxford University *Crystals for Windows* program.[9, 10] All non-hydrogen atoms were refined using anisotropic displacement parameters. After location of H atoms on electron-density difference maps, the H atoms were initially refined with soft restraints on the bond lengths and angles to regularise their geometry (C---H in the range 0.93--0.98 Å and U_{iso} (H) in the range 1.2-1.5 times U_{eq} of the parent atom), after which the positions were refined with riding constraints.[11] The final least-squares refinement converged to $R_1 = 0.0507$ ($I > 2\sigma(I)$, 4969 data) and $wR_2 = 0.0878$ (F^2, 7966 data, 622 parameters). The final CIF is available as supporting material, we note that the CheckCIF routine produced two alert B items, both related to the low resolution of the data set. Accordingly, the CIF file contains validation reply form items, which explain this issue in detail.

Figure S29. Fully labelled displacement ellipsoid (50%) of **5**.

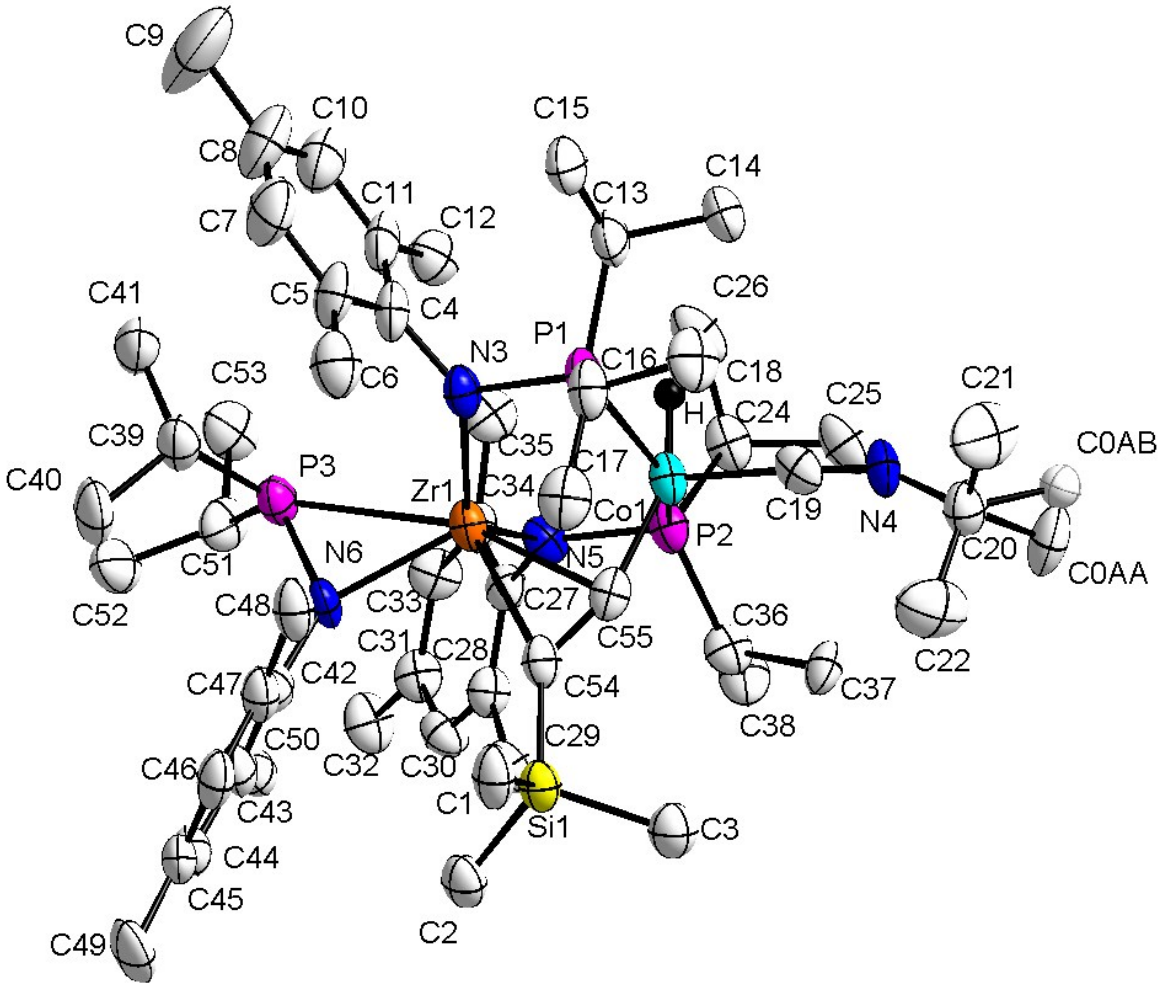

X-Ray data collection, solution, and refinement for 5. An orange plate like specimen of $C_{55}H_{94}CoN_4P_3SiZr$, approximate dimensions 0.285 mm x 0.198 mm x 0.144 mm, was coated with Paratone oil and mounted on a MiTeGen MicroLoop that had been previously attached to a metallic pin using epoxy for the X-ray crystallographic analysis. The X-ray intensity data were measured on a Bruker D8 Venture PHOTON II CPAD system equipped with a TRIUMPH curved-crystal monochromator and a Mo Kα fine-focus tube (λ = 0.71073 Å).

The frames were integrated with the Bruker SAINT software package[12] using a narrow-frame algorithm. The integration of the data using a monoclinic unit cell yielded a total of 87733 reflections to a maximum θ angle of 50.922° (0.83 Å resolution), of which 11572 were independent (average redundancy 7.58, completeness = 99.9%, R_{int} = 8.38%, R_{sig} = 5.53). The final cell

constants of a = 49.022(4) Å, b = 11.4685(9) Å, c = 25.848(3) Å, α =90°, β = 120.087(5)°, γ = 90°, volume = 12574(2) Å^3, are based upon the refinement of the XYZ-centroids of 9946 reflections above 20 $\sigma(I)$ with 2.88° < 2θ < 26.10°. Data were corrected for absorption effects using the Multi-Scan method (SADABS).[12] The ratio of minimum to maximum apparent transmission was 0.560. The calculated minimum and maximum transmission coefficients (based on crystal size) are 0.0094 and 0.0265.

The structure was solved and refined using the Bruker SHELXTL Software Package[13] within APEX3[12] and OLEX2,[14] using the space group $C2/c$, with Z = 8 for the formula unit, $C_{55}H_{94}CoN_4P_3SiZr$. Non-hydrogen atoms were refined anisotropically. Hydrogen atoms, were placed in geometrically calculated positions with U_{iso} = 1.2U_{equiv} of the parent atom (U_{iso} = 1.5 U_{equiv} for methyl). The final anisotropic full-matrix least-squares refinement on F^2 with 628 variables converged at R_1 = 10.69%, for the observed data and wR_2 = 13.15% for all data. The goodness-of-fit was 1.176. The largest peak in the final difference electron density synthesis was 1.27 e$^-$/Å^3 and the largest hole was -1.14 e$^-$/Å^3. On the basis of the final model, the calculated density was 1.147 g/cm^3 and F(000), 4632.0 e$^-$. There is one B-level alerts in the Checkcif that corresponds to obstruction of reflections by the beamstop. This was confirmed by independently reviewing the frames in which the missing reflections should have appeared. Electron density difference maps revealed that there was disordered solvent that could not be successfully modeled, so the structure factors were modified using the Olex2 BYPASS technique.[15] Olex2 reported a total electron density of 24.8 e$^-$ and total solvent accessible volume of 417 Å^3, likely corresponding to one ether molecule per unit cell.

References

1. B. P. Greenwood, G. T. Rowe, C.-H. Chen, B. M. Foxman and C. M. Thomas, *J. Am. Chem. Soc.*, 2010, **132**, 44-45.
2. J. P. Krogman, M. W. Bezpalko, B. M. Foxman and C. M. Thomas, *Dalton Trans.*, 2016, **45**, 11182-11190.
3. H. Zhang, G. P. Hatzis, C. E. Moore, D. A. Dickie, M. W. Bezpalko, B. M. Foxman and C. M. Thomas, *J. Am. Chem. Soc.*, 2019, **141**, 9516-9520.
4. N. O. Thiel, S. Kemper and J. F. Teichert, *Tetrahedron*, 2017, **73**, 5023-5028.
5. F. Cataldo, G. Strazzulla and S. Iglesias-Groth, *Radiat. Phys. Chem.*, 2009, **78**, 244-250.
6. O. Trhlíková, J. Zedník, J. Vohlídal and J. Sedláček, *Polym. Degrad. Stab.*, 2011, **96**, 1310-1320.
7. *Journal*, 2006.
8. A. Altomare, G. Cascarano, G. Giacovazzo, A. Guagliardi, M. C. Burla, G. Polidori and M. Camalli, *J. Appl. Cryst.*, 1994, **27**, 435-436.
9. C. K. Prout and L. J. Pearce, *Cameron*, Cambridge Crystallography Laboratory, Oxford, UK, 1996.
10. P. W. Betteridge, J. R. Carruthers, R. I. Cooper, K. Prout and D. J. Watkin, *J. Appl. Crystallogr.*, 2003, **36**, 1487.
11. R. I. Cooper, A. L. Thompson and D. J. Watkin, *J. Appl. Crystallogr.*, 2010, **43**, 1100-1107.
12. Bruker, *Saint; SADABS; APEX3.*, 2012, Madison, Wisconsin, USA.
13. G. M. Sheldrick, *Acta Cryst.*, 2015, **A71**, 3-8.
14. O. V. Dolomanov, L. J. Bourhis, R. J. Gildea, J. A. K. Howard and H. Puschmann, *J. Appl. Crystallogr.*, 2009, **42**, 339-341.
15. L. J. Bourhis, O. V. Dolomanov, R. J. Gildea, J. A. K. Howard and H. Puschmann, *Acta Crystallographica Section A*, 2015, **71**, 59-75.